Pendulum Simulation of Vehicular Impact on Retrofit Bridge Barriers

by

Geoffrey Tyler Mitchell, B.S.Ar.E.

Thesis

Presented to the Faculty of the Graduate School of

The University of Texas at Austin

in Partial Fulfillment

of the Requirements

for the Degree of

Master of Science in Engineering

The University of Texas at Austin

May 2005

Pendulum Simulation of Vehicular Impact on Retrofit Bridge Barriers

APPROVED BY
SUPERVISING COMMITTEE:

Richard E. Klingner

Eric B. Williamson

Acknowledgements

I would like to express my appreciation to Dr. Richard E. Klingner and Dr. Eric B. Williamson for their guidance and advice throughout the project. I have worked for Dr. Klingner as an undergraduate and graduate research assistant, and I must acknowledge that his wisdom and candor have taught more than I could ever express into words.

I also want to thank the technical staff of Ferguson Structural Engineering Laboratory: Dennis Fillip, Mike Bell, Blake Stassney, and Eric Schell. Every one of them made extraordinary efforts to help make my project successful. These people have taught me fabrication, workmanship and teamwork skills that I could not have otherwise obtained.

My thanks also go out to my undergraduate research assistants, Andy Chronister and Kyle Steuck. Their help and friendship are very much appreciated.

Finally to my mother, who is an unwavering example of determination, compassion, and perseverance. Thank you for everything.

May 6, 2005

Pendulum Simulation of Vehicular Impact on Retrofit Bridge Barriers

Geoffrey Tyler Mitchell, M.S.E.

The University of Texas at Austin, 2005

SUPERVISOR: Richard E. Klingner

The purpose of Research Project 0-4823 is to investigate how to replace a standard TxDOT bridge barrier after the original has been damaged by a vehicular collision. Post-installed mechanical anchors are a popular way to fasten structural members to hardened concrete and may be used for retrofit bridge barrier connection designs. The primary criterion for retrofit bridge barrier designs is that they perform similar to corresponding cast-in-place bridge barriers.

To understand how a standard cast-in-place T203 bridge barrier behaves during a vehicular impact, an impact test pendulum and a T203 bridge deck and barrier test specimen were developed and constructed at UT Austin's Ferguson Structural Engineering Laboratory (FSEL). The impact test pendulum currently serves as valuable tool for simulating the load history of a vehicular impact consistent with TL-3 testing criteria of *NCHRP Report 350*.

To validate the impact test pendulum, impact acceleration histories from rigid-barrier impact tests were compared with results from the crash test of a 1997 Geo Metro and finite-element analytical models using LS-DYNA, a widely used software package.

Table of Contents

viii

ix

List of Tables

List of Figures

CHAPTER 1

Introduction, Objectives and Scope

1.1 INTRODUCTION

The purpose of TxDOT Research Project 0-4823 ("*Performance Testing of Anchors for Retrofitting and Repair of Bridge Barriers*") is to find out how to design replacement bridge barriers after the original barrier has been damaged by vehicular impact. A widely used and effective way to connect structural components to hardened concrete is to use post-installed anchors. The goal of this research project is to determine how to use these anchors to replace damaged bridge barriers by retrofits with suitable performance retrofits. Additionally, the use of anchors is also applicable for pre-cast bridge barrier applications. In TxDOT documents, bridge barriers are commonly referred to as both bridge "barriers" and "rails." In this thesis, they are referred to as "barriers."

In this study, tests are conducted on full-scale bridge deck and barrier specimens to determine the behavior of TxDOT standard cast-in-place and retrofit barrier designs. The retrofit bridge barrier designs will use through-bolt anchor configurations to fasten the barrier to the bridge deck. After the behavior of the retrofit bridge barriers is characterized and evaluated, the best-performing connection detail will be submitted to TxDOT for implementation.

Project 0-4823, funded by Texas Department of Transportation (TxDOT) through the Center for Transportation Research (CTR), addresses retrofit approaches using mechanical post-installed anchors. A related research project, supported by TxDOT through the Texas Transportation Institute (TTI), addresses retrofit approaches using adhesive post-installed anchors.

1.2 OBJECTIVES

The following subsections outline the objectives of Research Project 0-4823 and of this thesis.

1.2.1 Objectives of Project 0-4823

Deliverables for Project 0-4823 include design guidelines and documentation for the retrofit of TxDOT standard bridge barriers, including the following:

o   recommendations for patterns and spacing of mechanical anchors based on constructability, structural performance and behavior of the bridge barrier;

o   clearly defined field installation methods for barrier retrofits;

o   recommend limits for design based on failure modes of bridge barriers and mechanical anchor behavior; and

o   documentation presenting the research methodology, execution and results.

At the conclusion of Project 0-4823, researchers at the University of Texas will be able to characterize and predict the behavior of TxDOT standard bridge barriers (and various barrier retrofit schemes) subjected to vehicular impact loads. This new level of understanding will facilitate the development of improved bridge barrier design tools for TxDOT engineers, and also supplement the current state-of-the-art of bridge barrier impact testing.

1.2.2 Objectives of this Thesis

The objective of this thesis is to document research conducted by the author for Research Project 0-4823. Included in this research are the development and validation of an impact test pendulum setup to simulate a vehicular impact against a bridge barrier.

Development of the impact test pendulum setup includes the following steps:

o   review literature relevant to the state-of-the-art of bridge barrier testing;

o   identify logistical and operational concerns regarding a large impact test pendulum setup; and

o   design and fabricate the impact test pendulum setup.

Validation of the impact test pendulum setup includes the following tasks:

o   design deformable "crush packages" to simulate the crushing characteristics of a specific production-model vehicle;

o   develop instrumentation to record the results of a impact-pendulum testing; and

o   compare analytical, crash-test, and pendulum-impact test data to verify that the impact test pendulum adequately simulates a vehicular collision to *NCHRP Report 350* criteria, (NCHRP Report 350 1993).

An additional objective of the author is that this thesis serve as a background resource for future researchers involved in Project 0-4823.

1.3 SCOPE

The following subsections outline the scope of Research Project 0-4823 and of this thesis.

1.3.1 Scope of Project 0-4823

Researchers at UT Austin are using pendulum impact testing and finite-element analytical models to evaluate the performance of bridge barriers.

The development and validation of the impact test pendulum setup is within the scope of this author's research, whose objectives are outlined in Section 1.2.2.

The development of finite-element analytical models, created with LS-DYNA, falls within the scope of Graduate Research Assistant Megan Tolnai. Finite-element models are used to simulate pendulum impact tests and full-scale crash tests with TxDOT bridge barriers (Tolnai 2005).

Finally, the testing of TxDOT standard bridge barrier specimens and the creation of deliverable documentation, listed in Section 1.2.1, falls within the scope of future researchers of Project 0-4823, who will use the impact test pendulum setup and analytical models to test and validate bridge barrier retrofit designs with mechanical post-installed anchors.

1.3.2 Scope of this Thesis

This thesis addresses background information and the development of an experimental testing program.

Chapter 2 outlines the state-of-the-art of mechanical anchor connection design and testing standards for bridge barriers in the United States. The development of a bridge deck and barrier test specimen is described in Chapter 3,

and the design and validation of the impact test pendulum are explained in Chapters 4 and 5 respectively. Finally, Chapter 6 contains a summary, conclusions, and recommendations based on the author's research for Project 0-4823.

CHAPTER 2
Background

2.1 MOTIVATION FOR BACKGROUND RESEARCH

The goal of Project 0-4823 is to design a retrofit bridge barrier that performs like the corresponding cast-in-place barrier during vehicular impact. At the beginning of the research, this goal presented three main challenges to the researchers of Project 0-4823:

o   develop a connection design, using mechanical anchors, to anchor a retrofit bridge barrier to a concrete bridge deck; and

o   develop a testing program to characterize and evaluate the performance of bridge barriers; and

o   design an appropriate retrofit bridge barrier.

To develop a sufficient knowledge base from which to address these challenges, the researchers on Project 0-4823 reviewed the state-of-the-art of mechanical anchor connection design, and bridge barrier testing standards. Salient results of that review are summarized here.

2.2   DESIGN OF CONNECTIONS USING MECHANICAL ANCHORS

The design of retrofit bridge barrier connections using mechanical anchors requires a functional understanding of the behavior of mechanical anchors under direct tension. While mechanical anchors are also commonly referred to as "fasteners," the term "anchors" is used in this thesis.

Design and behavior guidelines for mechanical anchors are outlined in Appendix A, which is excerpted and updated from *"Behavior and Design of Fastening to Concrete"* (Klingner 2003).

2.3   THE STATE-OF-THE-ART OF BRIDGE BARRIER TESTING

To develop a bridge barrier testing program, it is necessary to understand relevant testing standards. Those are discussed in the following sections.

2.3.1   Overview of Testing Standards for Bridge Barriers

The TxDOT bridge barriers under consideration for Project 0-4823 include TxDOT Types T203 and T501, shown in their normal cast-in-place form, in standard bridge deck configurations, in Figure 2.1(a) and (b) respectively.

(a)   (b)
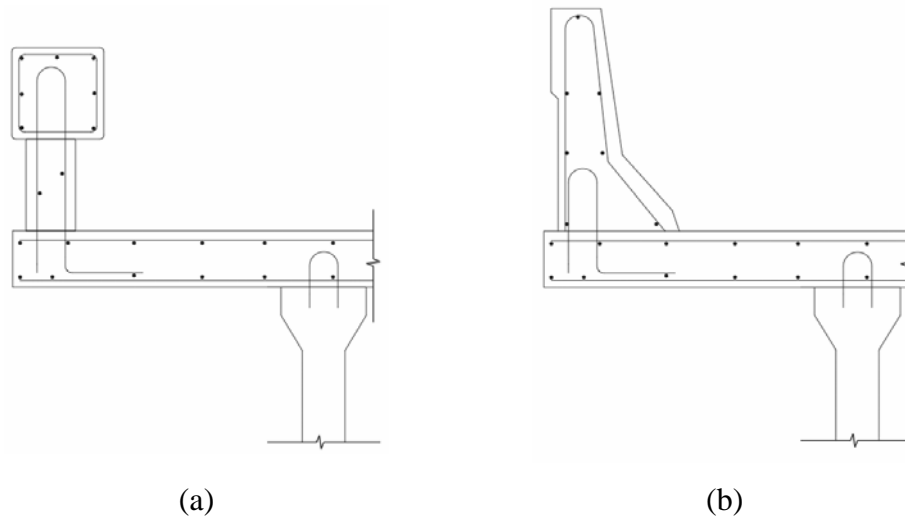
Figure 2.1-Transverse sections of the (a) T203 and (b) T501 bridge barriers

The National Cooperative Highway Research Program (NCHRP) regulates the testing of highway bridge barriers throughout the United States. *NCHRP Report 350* (1993) prescribes testing procedures and evaluation criteria for bridge barriers. Bridge barrier designs to be installed on highways receiving any federal funding (in practical terms, on any federal or state highway) must be crash-tested in accordance with *NCHRP Report 350* and must pass that document's required performance criteria. *NCHRP Report 350* applies to all longitudinal barriers, including the T203 and T501 bridge barriers that are the subject of Project 0-4823.

A longitudinal barrier has two functions: 1) prevent penetration of the barrier by a vehicle; and 2) redirect a vehicle without causing it to flip, vault or snag on the barrier. For any longitudinal barrier to pass a NCHRP test, it must satisfy criteria based on both of those functions. Final evaluation of a longitudinal barrier is ultimately accomplished by a full-scale crash test of a moving test vehicle against a specified length of longitudinal barrier, using parameters that are also prescribed in *NCHRP Report 350*.

8

2.3.2 Test Criteria of *NCHRP Report 350* TL-3

NCHRP Report 350 prescribes six test levels for evaluating longitudinal barriers against vehicular impact. Project 0-4823 is concerned with Test Level 3 (TL-3) criteria because the T203 and T501 bridge barriers have been designed, tested, and validated using a TL-3 crash test. NCHRP TL-3 crash-test criteria are outlined in Table 2.1.

Table 2.1 NCHRP Report 350 TL-3 criteria (NCHRP 1993)

Test Level	Mass of Vehicle	Nominal Speed	Angle of Impact	Impact Energy
TL-3	820 ± 25 kg	100 ± 4 km/h	$20 \pm 1.5°$	37 ± 3 k-J

Figure 2.2 illustrates the TL-3 criteria of *NCHRP Report 350.* Because full-scale crash testing is very expensive, *NCHRP Report 350* permits the use of "surrogate vehicles" to simulate vehicular impact loads when only strength and stiffness of bridge barriers are being evaluated. To be acceptable as a surrogate vehicles for TL-3 testing, the surrogate must deliver an impact equivalent to that associated with the component perpendicular to the plane of the bridge barrier from a TL-3 NCHRP crash test (Figure 2.2). Acceptable surrogate vehicles include impact pendulums and four-wheeled bogies.

9
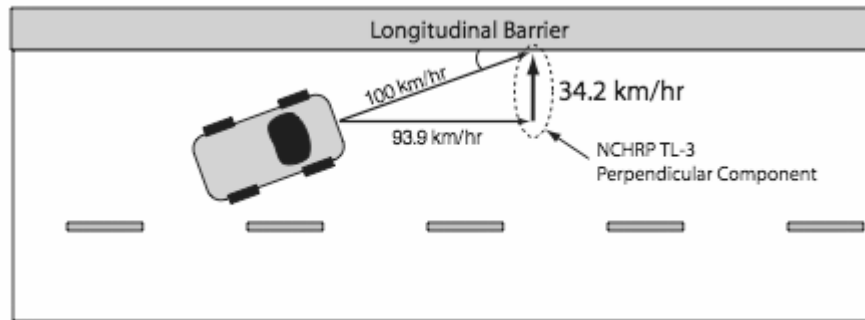
Figure 2.2- NCHRP Report 350 TL-3 crash-test criteria

A full-scale TL-3 crash test addresses the behavior of a test vehicle as well as the barrier. Because the objective of Project 0-4823 concerns equivalency of performance of the T203 and T501 barriers only, it is not necessary to use an actual vehicle, and a surrogate vehicle is satisfactory. In this study, that surrogate vehicle is an impact test pendulum.

CHAPTER 3

Design of T203 Bridge Deck and Barrier Test Specimen

3.1 INTRODUCTION

In this thesis, a test specimen consisting of a TxDOT bridge deck with a T203 bridge barrier is referred to, for convenience, as a "T203 bridge deck and barrier test specimen," whose purpose is to allow researchers at UT Austin to observe the behavior of cast-in-place and retrofit TxDOT T203 bridge barriers subjected to a NCHRP TL-3 impact. To achieve the best possible simulation of actual bridge deck and barrier construction, researchers used TxDOT design drawings and design standards to design a test specimen incorporating a full-scale T203 barrier mounted on a reinforced concrete deck.

Figure 3.1- T203 bridge deck and barrier specimen at FSEL

3.2 DESIGN CRITERIA FOR T203 TEST SPECIMEN

Design criteria for the development of the T203 bridge deck and barrier specimen include the following:

o   the specimen must be capable of representing retrofit as well as cast-in-place barriers,

o   the specimen must include relevant details of the T203 barrier and the standard TxDOT 3-ft (0.9-m) bridge deck overhang;

o   the specimen must fit into the impact test pendulum setup whose design is described in Chapter 4 of this thesis; and

o   the specimen must incorporate details permitting the retrofit barrier to be attached to the bridge deck.

3.2.1 Relevance of Test Specimen for Retrofit and Cast-in-Place Bridge Barriers

The bridge barrier specimen is designed to accommodate both cast-in-place and retrofit bridge barriers. Cast-in-place T203 barrier specimens are constructed by casting stirrups into the T203 bridge deck specimen (Figure 3.2), and then later casting the T203 bridge barrier specimen over the stirrups. Retrofit bridge barrier specimens are attached by drilling or coring into the bridge deck specimen and installing mechanical anchors, either into the deck or through it.

***Figure 3.2- Reinforcement layout of the T203 bridge deck and cast-in-place
barrier test specimens***

3.2.2   Relevant Details of T203 Barrier and Deck Overhang

The reinforcing details of the T203 bridge deck and barrier test specimen
were taken directly from TxDOT design documentation (TxDOT 2003).   An
important criterion for the T203 bridge deck and barrier specimen is that it
include the standard TxDOT overhang usually used on TxDOT bridges.   This
overhang extends 3 ft (0.9 m) from the outside bridge girder, which is connected
to the bridge deck via U-bars (extensions of girder transverse reinforcement)
during casting (Figure 3.3(a)). To reproduce those boundary conditions in the test
setup, the T203 bridge deck and barrier test specimen incorporates a 3-ft (0.9-m)
cantilever overhang whose base is tied to the laboratory strong floor with threaded
steel rods Figure 3.3(b).

(a)   (b)
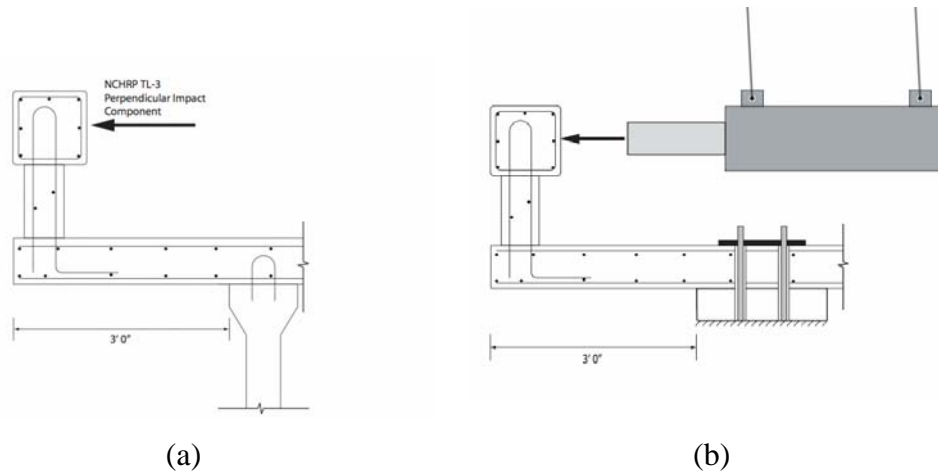
Figure 3.3(a)- Schematic of T203 bridge barrier in a typical highway
configuration, and (b) bridge deck and barrier specimen at FSEL

3.2.3   Relevant Dimensional Compatibility between Specimen and Impact Test Pendulum

The T203 bridge deck and barrier specimen was also required to fit within the impact test pendulum setup at Ferguson Laboratory. Figure 3.4 shows a model of the specimen within the pendulum's support frame. Each specimen has two bridge barriers, one at each end. After the first barrier is tested (Figure 3.4), the specimen can be lifted with an overhead crane and rotated 180 degrees to test the barrier at the other end.
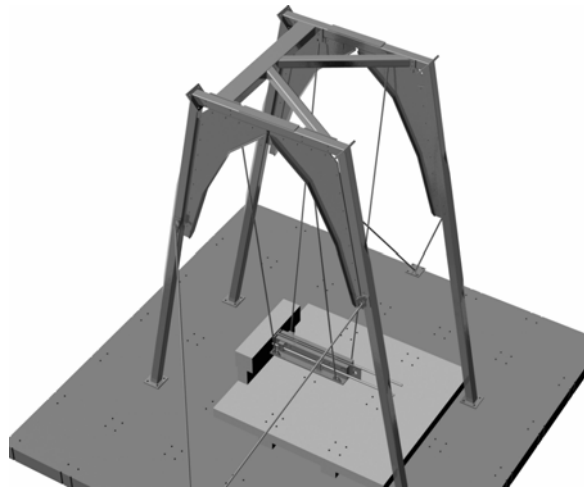
Figure 3.4- impact test pendulum withT203 test specimen in place

3.2.4 Relevant Details for Attachment of T203 Retrofit Bridge Barrier to Deck of Specimen

In designing the T203 retrofit bridge barrier test specimen, special attention was paid to ensure that it could accommodate a wide variety of possible retrofit barrier connection details using mechanical post-installed anchors.

Using the anchor connection design provisions of ACI 318-05 Appendix D, the capacity of the bridge deck overhang as governed by concrete breakout around the anchors was estimated in terms of the number of anchors used to connect a T203 retrofit bridge barrier to the deck. The T203 bridge barrier has either a continuous lower portion of prescribed thickness, or intermittent lower portions 5-ft (1.5-m) long and the same prescribed thickness. Based on the dimensions specified by TxDOT, the footprint of the barrier on the deck is prescribed in size. Breakout capacity of the anchor group does not increase much as more anchors are added, because of increasing overlap among the concrete breakout bodies associated with each anchor (Appendix A). This is shown in

Figure 3.5, which suggests that the tensile breakout capacity of the bridge deck is limited to about 78 kips (347 kN), regardless of the number of anchors used.

Concrete Breakout Capacity vs Number of Anchors
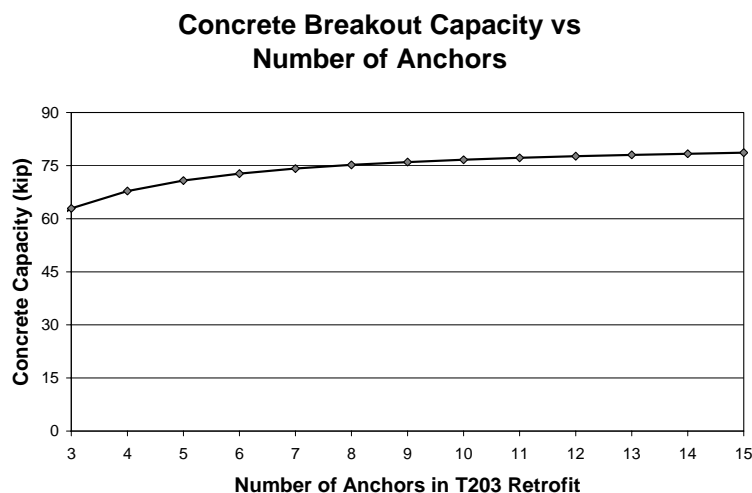
Figure 3.5- Tensile breakout capacity of concrete bridge deck as a function of anchors used to connect T203 retrofit bridge barrier to overhang

Based on this relationship, the researchers of Project 0-4823 concluded that eight anchors would be an appropriate upper bound for a T203 retrofit barrier connection design. The barrier of the T203 retrofit specimen (Figure 3.6(a)) was therefore designed with eight vertical PVC ducts, shown in Figure 3.6(b), to accommodate any reasonable combination of threaded rods, which would then be attached to the underlying deck, using either mechanical anchors or through-bolts.

<div align="center">

(a)   (b)
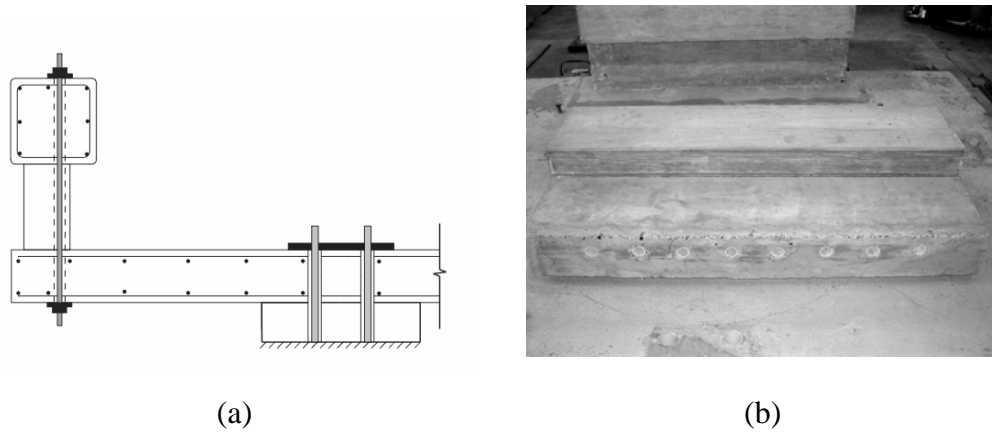
Figure 3.6(a)-Schematic of T203 retrofit specimen and (b) T203 retrofit bridge barrier with PVC ducts for anchors

</div>

3.3   INSTRUMENTATION OF SPECIMEN

The ability of UT Austin researchers to evaluate the performance of the T203 bridge barrier depends on the instrumentation scheme developed for the test specimen. To understand the impact performance of a T203 bridge barrier, the following must be known:

o   impact force;
o   bridge barrier and deck stresses; and
o   bridge barrier and deck displacements.

Measurement of impact force is discussed in Chapter 5, and the measurement of displacements and stresses is briefly discussed in this section.

To measure stresses in the T203 bridge deck and barrier test specimen, a large number of electrical resistance strain gages were installed on steel

<div align="center">

17

</div>

reinforcing bars prior to casting concrete. For the bridge deck, strain gauges were installed on tension-side reinforcing bars near anticipated yield lines in the bridge deck near the interface with the T203 bridge barrier. These strain gages are expected to give researchers data regarding the propagation of stresses within the bridge deck during a pendulum impact test.

Strain gauges are also installed on reinforcing bars at the tension face of the T203 bridge barrier specimen. These gages are expected to help researchers determine the stress level of the reinforcement at concrete breakout. This stress information will be extremely valuable in confirming that CC Method (described in Appendix A) gives accurate predictions of anchor capacity as governed by concrete breakout, under TL-3 impact loads.

Finally, linear variable differential transformers (LVDT) are to be installed underneath the bridge deck overhang of the test specimen to capture displacements and rotations of the bridge deck and barrier specimens during a pendulum impact test. The data obtained from the LVDT's can be used to estimate impact energy absorption characteristics of the bridge deck and the T203 bridge barrier specimens.

3.4 CONCLUDING REMARKS ON DEVELOPMENT OF T203 BRIDGE DECK AND BARRIER SPECIMEN

The T203 bridge deck and barrier test specimen was designed to allow researchers at UT Austin to evaluate the behavior of cast-in-place and retrofit TxDOT T203 bridge barriers subjected to a NCHRP TL-3 impact. By consulting TxDOT design documentation and considering geometric compatibility with the

impact test pendulum, the T203 bridge deck and barrier specimen is expected to permit an accurate and efficient bridge barrier testing program.

CHAPTER 4

Design of Impact Test Pendulum

4.1   INTRODUCTION

To evaluate the structural performance of TxDOT standard bridge barriers and the associated retrofit variants of those barriers, UT Austin researchers developed a testing program with accurately simulated vehicular impact loads.

To apply those loads, the researchers decided on an impact test pendulum, consisting of a pendulum mass, supported on cables from a supporting frame (Figure 4.1). The design, development and construction of that pendulum, carried out at The University's Ferguson Structural Engineering Lab (FSEL), took five months during the academic year 2004-2005, and is described in this chapter. Design of the pendulum addressed the structural performance of the frame itself, and also many other parameters, including constructability, cost, laboratory resources, and the steep learning curve for the novice designer/fabricator who also authored this thesis.
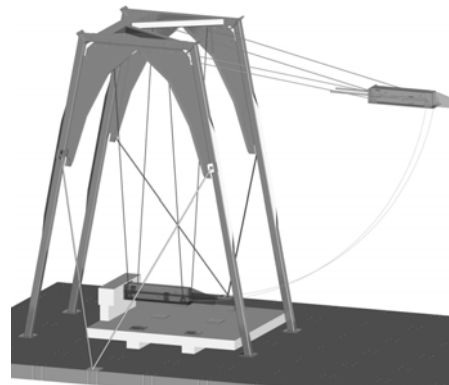
(a)   (b)

Figure 4.1(a) and (b)- Impact test pendulum at UT Austin

4.2 OPERATIONAL OVERVIEW OF IMPACT TEST PENDULUM

Ferguson Laboratory's impact test pendulum is designed to simulate a vehicular impact against a bridge barrier. The entire test setup consists of an 855-kg pendulum mass, supported on four cables from a 22-ft (6.7-m) tall steel frame, and which can be released to fall through a 16-ft (4.9-m) drop height. The pendulum mass and drop height are specifically designed to conform to Test Level 3 (*NCHRP Report 350*, 1993) criteria for longitudinal barriers, reviewed in Chapter 2 of this thesis.

Figure 4.2 shows the principal components of the impact test pendulum at FSEL, and how it works. Using a steel lifting cable, the pendulum mass is raised by an electric winch and pulley, attached to a pendulum mass lifting frame, to the desired height. To start a test, a pneumatic latch on the pendulum is actuated, releasing the pendulum from the lifting cable. After the cable is released, the pendulum mass falls along a circular path and impacts the test specimen.
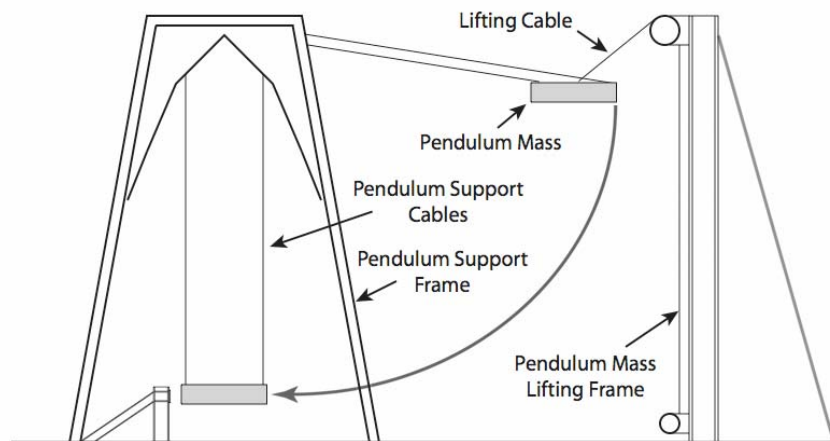
Figure 4.2- Principal components of the impact test pendulum at FSEL, and how it works

In addition to the obvious components required to raise and release the pendulum mass, other components of the impact test pendulum setup are also significant, particularly the deformable, steel-tube "crush packages" that are installed on the frontal impact zone of the pendulum mass. The characteristics of these crush packages can be varied to simulate vehicle-specific impact characteristics. Figure 4.3 shows a schematic of a T203 barrier test specimen and the pendulum mass with a crush package installed. Development and behavior of the crush packages are discussed in Chapter 5.

The pendulum setup permits testing barriers up to 10-ft (3.0-m) wide (perpendicular to the swing orientation of the pendulum), including a simulated TxDOT bridge deck and its commonly associated 3-ft (0.9-m) cantilever deck overhang (Figure 4.3(a)). Because it can accommodate a wide range of barrier and deck specimens, and because its crush package can be adjusted to obtain a wide range of impact acceleration histories, this setup can simulate virtually any *NCHRP Report 350* TL-3 impact scenario.

(a)   (b)
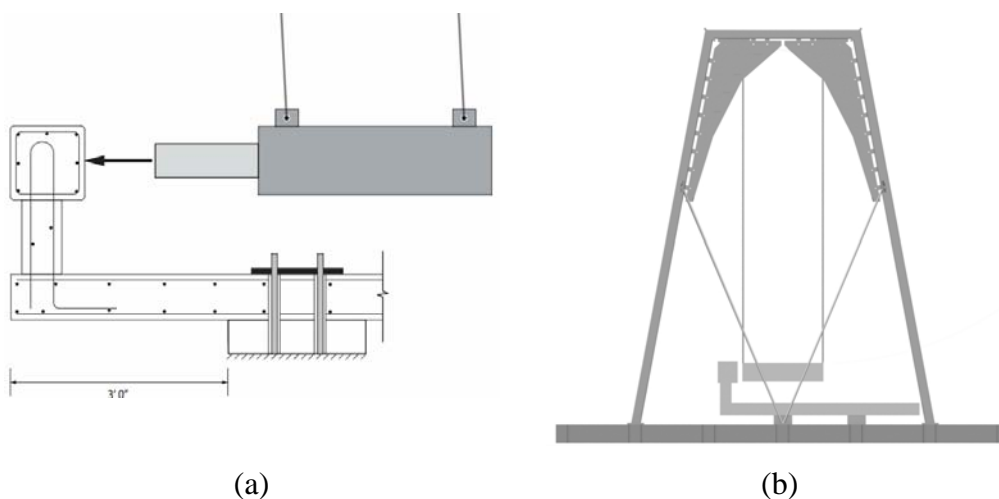
Figure 4.3(a)- T203 bridge deck and barrier test specimen with pendulum mass and (b) their position within pendulum support frame

22

4.3   DESIGN PROCESS FOR PENDULUM TEST SETUP FOR STUDY 0-4823

Initially, UT Austin researchers considered using high-speed hydraulics to simulate the impact loading of a vehicular collision. In initial feasibility studies, however, it was concluded that the required impulse could be generated more cost-effectively using an impact test pendulum, which (as discussed in Chapter 2) is accepted by *NCHRP Report 350* as a "surrogate vehicle" to simulate vehicular impact loads.

4.3.1   Initial Design Concepts for Impact Test Pendulum

Design of the FSEL impact test pendulum, like many design processes, was iterative. Many concepts were developed, evaluated and discarded, and the lessons learned from those initial false steps were incorporated into subsequent designs.

Early in the design process, as primary design criteria were established, considerable emphasis was placed upon the ability to perform multiple tests in quick succession, using a self-reacting setup that could be placed anywhere in the Ferguson Laboratory. The initial concepts in Figure 4.4 include a self-reacting test setup with four T203 specimens and a steel frame capable of being lifted and rotated at 90-degree increments.

| (a) | (b) |
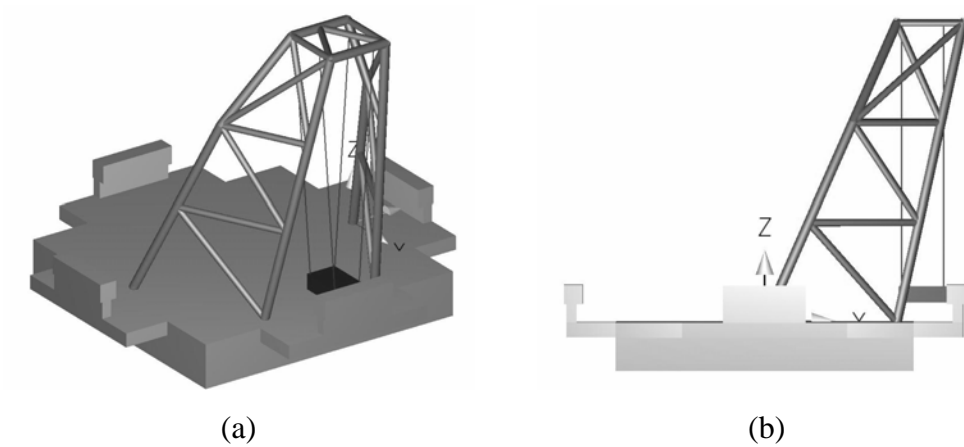
***Figure 4.4(a) and (b)- Initial concepts in the design of a multi-directional
impact test pendulum***

The designs of Figure 4.4 were eventually discarded, for several reasons:

o   The weight of the four-sided concrete specimen would have exceeded the
    capacity of the FSEL's overhead crane, and the tested specimens would
    have had to be cut up and removed from the lab in pieces. This would
    have been undesirable, requiring a large labor force and a large and
    potentially dangerous concrete saw.

o   Given the multi-directional nature of this setup, it wasn't clear how the
    pendulum mass could best be lifted and released along four perpendicular
    orientations. The device for lifting the pendulum mass had not yet been
    developed, and this setup would have required an unacceptably large plan
    footprint on the laboratory floor.

o   Safety concerns existed regarding the four testing orientations implied by
    this design.

It was ultimately decided to have a single, well-established swing orientation, and a single corresponding orientation for the necessary system to contain the debris created by impact of the pendulum mass with the barrier specimen. Because the requirement that the setup be self-equilibrating was not crucial, the pendulum support frame would be bolted to the laboratory strong floor. Each test specimen would accommodate only two barriers; would be bolted to the laboratory strong floor within the pendulum support frame; and would be oriented parallel to the swing plane of the pendulum mass.

4.4 FINAL DESIGN OF PENDULUM SUPPORT FRAME

The largest and most complex component of the impact test pendulum at FSEL, and also the hardest component to design, is its 22-ft (6.7-m) tall pendulum support frame. The frame had to perform satisfactorily as part of the test setup, and also be cost-effectively built and erected at FSEL. Performance criteria included sufficient resistance to design loads, and sufficient stiffness to limit deflections under those loads. In this section, its design to meet each of those objectives is discussed, followed by discussion of constructability and fabrication issues.

4.4.1 Design Loads for Pendulum Support Frame

Unlike traditional live loads, the design loads imposed by a swinging pendulum mass on its associated support frame are consistent and can be calculated using basic physics. The support frame is loaded only by the tension in the cables supporting the pendulum mass. Two cases are of interest: when the pendulum is swinging freely; and when the pendulum is held at its initial drop height by the lifting cable. Each case is discussed below.

25

When the pendulum is swinging freely, cable tension depends on two things only: 1) the mass of the pendulum; and 2) the swing radius of the pendulum mass (that is, the cable length). Figure 4.5(a) shows the physical relationship between the cable tension, pendulum mass, and swing radius in a free-body diagram. From the equilibrium expression in Figure 4.5(a) it can be shown that increasing the pendulum mass and reducing the swing radius effectively increases the cable tension. Figure 4.5(b) shows the application of this relationship with respect to the loads experienced by the pendulum support frame.

$$\sum \vec{F} = m \cdot \vec{a}$$

$$\left(F_{tension} - mg\sin\theta\right) = m \cdot a_{centripetal} = \frac{m \cdot v^2}{r}$$

(a)

Pendulum Support Frame Loads
(Due to Swinging Pendulum Mass)
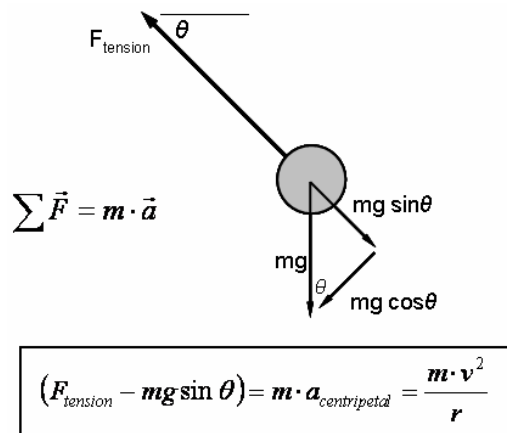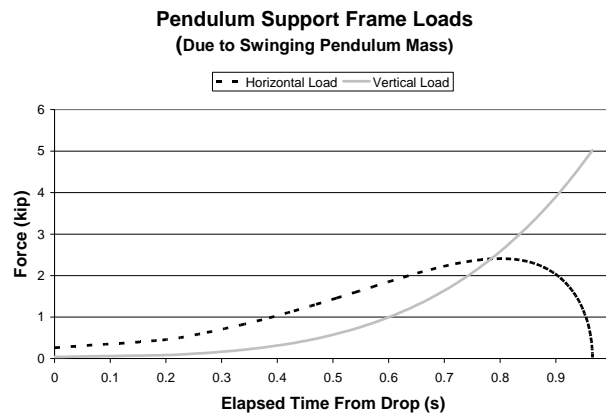
(b)

Figure 4.5(a)- Freebody of swinging pendulum mass, and (b) corresponding loads experienced by the pendulum support frame

When the pendulum is supported at its initial drop height, the cable tension depends again on two things only (but not the same two as before): 1) the mass of the pendulum; and 2) the initial angle required to achieve the desired drop height. Coincidentally, the swing radius is also important in this case, because it determines the initial angle from the vertical at which the pendulum mass must be

27

supported to achieve a desired drop height. Figure 4.6 shows two pendulums with
the same mass and the same drop height Δ , but at different initial cable angles.
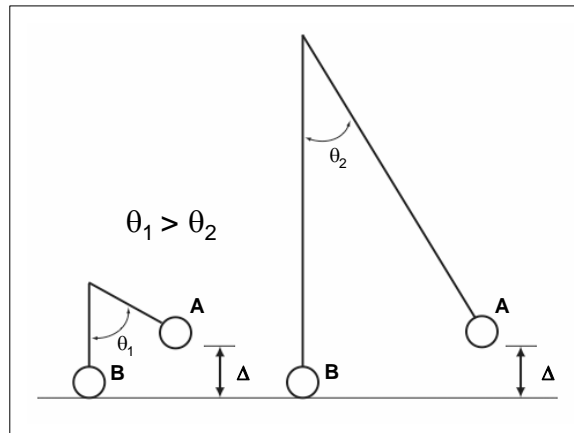
Figure 4.6- Relationship between swing radius and initial angle of pendulum support cables

Although the total energy of the two systems is identical, the pendulum on
the left has a larger cable tension before it is dropped because it is held at a larger
angle from the vertical than the pendulum on the right. Figure 4.7(a) shows a free
body of a pendulum mass held at its initial drop height.

$$F_{pendulum\_cable} \sin \theta_1 + F_{lifting\_cable} \sin \theta_2 = mg$$
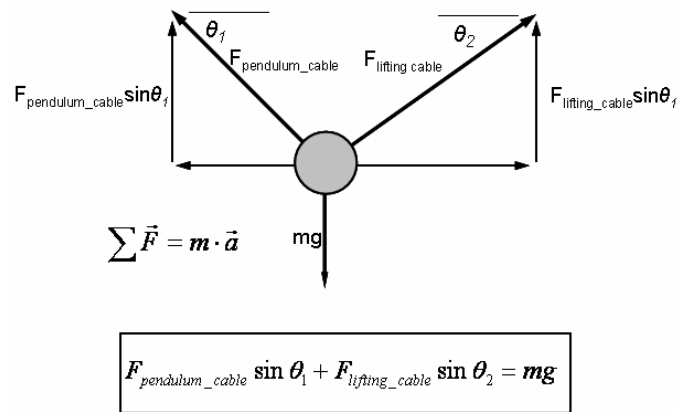
Figure 4.7- Free body of pendulum mass supported at the initial drop height by the lifting cable

Structural analysis of the pendulum support frame determined that its critical loading case is just before release of the pendulum. This is critical because it generates the highest lateral load (7 kip) on the pendulum support frame. The maximum load conditions associated with both pendulum mass loading conditions are summarized in Table 4.1, while (b) shows the deformed shape of the pendulum support frame subjected to the critical loading case.

Table 4.1 Maximum pendulum support frame loads associated with both pendulum mass loading conditions

Load Case	Maximum P_x	Maximum P_y
Pendulum Mass Swinging	approx. 2.5 kip	approx. 5 kip
Pendulum Mass Supported at Drop Height	approx. 7 kip	approx. 1 kip

Figure 4.8- Analytical model of the deformed shape at maximum design load

4.4.2 Structural Design of Pendulum Support Frame for Loads and Deformations

In addition to design for strength, a lateral deflection limit of 0.10 in. was imposed on the design of the pendulum support frame. This requirement was decided upon by the supervisors of Project 0-4823 in an effort to ensure a stable, safe design.

The structural design of the pendulum support frame was checked for strength and deflection limits by using the following analyses: 1) static elastic analysis; 2) modal dynamic elastic analysis; 3) elastic stability analysis; and 4) inelastic limit-state analysis on various connection details. Structural analysis programs used included SAP 2000 and MASTAN 2. The deflection limit invariably controlled the design.

4.4.3 Design of Pendulum Support Frame for Construction Compatibility

To ensure that fabrication and constructability problems did not detract from the success of the pendulum support frame, its design was checked using three-dimensional computer modeling techniques.

Structural analysis computer programs were used to assess structural performance, and non-structural, solid modeling programs, such as Microstation 8, were used to ensure that the pendulum support frame could be easily built. Throughout the design process, the entire impact test pendulum setup, including the T203 test specimen, pendulum mass lifting frame, pendulum mass, and laboratory strong floor grid, were detailed in the computer to determine geometric compatibility. As anticipated, many potential problems were identified and solved in this virtual three-dimensional computer environment before any structural steel was ordered. These efforts were validated after erection of the pendulum support frame, because no procurement, constructability, or fabrication problems arose during construction.

4.4.4 Laboratory Resources for Design of Pendulum Support Frame

Understanding the fabrication resources and capabilities of FSEL was critical in determining an appropriate design for the pendulum support frame. These resources are briefly discussed in this section.

The most notable fabrication resource at FSEL is its large selection of steel-cutting band saws and torches, hydraulic steel punches, and welding equipment. The author had to be mindful of the size and capacity of each one of these machines when designing member sizes and connection details. The preliminary design phase of the pendulum support frame involved much

31

discussion with the technical staff of FSEL to determine which design concepts would be most feasible.

In addition to fabrication resources, FSEL also has a 25-ton capacity overhead crane to move and erect structural steel sections. Although this crane was invaluable to the erection of the pendulum impact frame, it was also a design constraint. As explained in Section 4.4.1, the swing radius of the pendulum mass has a large influence on the design loading of the pendulum impact test frame. It was beneficial to make the pendulum impact test frame as tall as possible, to increase the swing radius and thus reduce the design loading. The maximum height of the crane hook, however, limited the design height of the frame to 22 ft (6.7 m).

The design of the pendulum support frame was the best attempt by the author to use the facilities available at Ferguson Lab. Each piece of equipment had capabilities and limitations that needed to be considered so that the pendulum impact frame could be successfully constructed as designed.

Finally, to complement the fabrication resources at FSEL, the technical staff was willing to train the author on any piece of equipment available at the laboratory. As a result, it was possible for the pendulum support frame to be completely fabricated and erected by the researchers of Project 0-4823. This was a great advantage because it facilitated a swift construction schedule and a relatively low monetary cost for the pendulum support frame.

4.4.5   Fabrication and Erection of Pendulum Support Frame

Fabrication of the pendulum support frame began July 1, 2004 and was completed in one month. During fabrication and erection, it became clear that pre-construction efforts, using three-dimensional modeling to anticipate and eliminate constructability problems in advance, had circumvented many potential fabrication and erection pitfalls. Appendix B shows selected three-dimensional design models and the construction documentation generated from them.

Figure 4.9- Pendulum support frame under construction at FSEL

Figure 4.9 shows the pendulum support frame under construction on the lab floor of FSEL. The frame was broken up into three major components: two planar arches, and a large K-brace to tie the structure together. Each of these components was clamped together and welded on the floor of the lab to ensure proper alignment. After all three major components were fabricated and painted, the frame was erected piece by piece using FSEL's overhead crane. The frame was then plumbed, and its structural bolts tightened with a pneumatic impact wrench. The final stage of construction was the procurement and installation of the steel cables necessary for operation of the impact test pendulum.

4.5   DESIGN OF PENDULUM MASS AND ASSOCIATED COMPONENTS

Although the primary criterion of the pendulum mass is to provide sufficient mass to satisfy *NCHRP Report 350* impact-energy criteria, significant design effort was necessary to ensure that the pendulum mass would be a consistent, reusable component of the impact test pendulum.

Figure 4.10- Pendulum mass

In the early stages of the design of the pendulum mass, the decision was made to create the pendulum mass as a modular system of steel plates. Steel was chosen for the following reasons:

o   its high density would lead to a reasonably compact geometry for the pendulum mass;

o   its strength, toughness and ductility would lead to the ability to survive repeated bridge barrier impacts; and

o   its workability and weldability would facilitate fabrication of the pendulum mass at Ferguson Laboratory.

Recognizing that the impact test pendulum might be used for other future research projects with different requirements for pendulum mass, project researchers decided on a modular pendulum mass system composed of steel plates, bolted to a central supporting support chassis consisting of a built-up tee section.

In addition to the central chassis and the plates bolted to it, other components of the pendulum mass include the following:

o   plate anchors to attach the support chassis to the support cables; and

o   a pneumatic release latch, bolted to the support chassis at the center of gravity of the pendulum mass, and connected (when the latch is closed) to the lifting cable.

These other components are shown in Figure 4.10, which shows the pendulum mass hanging from its support cables within the pendulum support frame. Although the pendulum mass itself was designed and fabricated by the author, the pneumatic release latch is a special component of the pendulum mass system that deserves special mention (Figure 4.11).
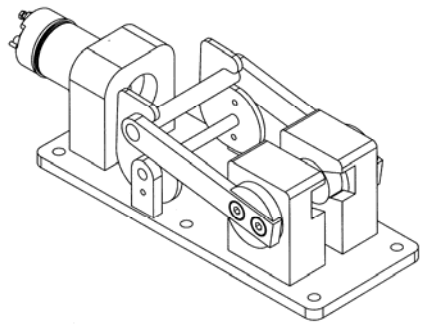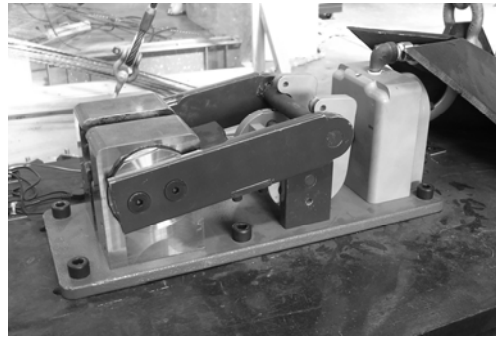
(a)   (b)

Figure 4.11(a) and (b)- Pneumatic release latch for pendulum mass[1]

After the design and erection of the impact test pendulum setup, it remained unclear how the pendulum mass could be released after being raised to the proper drop height. After much consideration, and two failed prototypes, it became clear that the design of a mechanism that could quickly and safely release a cable under high tension was not a trivial problem.

While the author was attempting to develop a third prototype, an FSEL laboratory technician volunteered his expertise in component development and machining. The result of his design and fabrication efforts is a pneumatically-actuated latch capable of releasing the pendulum mass safely and consistently. This extraordinary level of effort and generosity on behalf of the laboratory staff at FSEL is noteworthy, and very much appreciated by the author.

---

[1] Design drawing prepared by Dennis Fillip, FSEL, 2004.

4.6 DESIGN OF PENDULUM MASS LIFTING FRAME

The final component of the impact test pendulum to be designed was the pendulum mass lifting frame. Although it had the most straightforward structural requirements of any component of the impact test pendulum setup, its structural and mechanical design still involved notable challenges, discussed in this section.
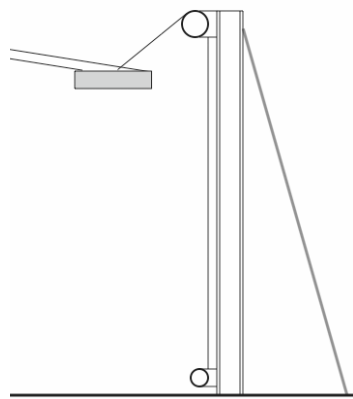
(a)   (b)

Figure 4.12(a) and (b)- Pendulum mass lifting frame at FSEL

4.6.1 Design Loads for Pendulum Mass Lifting Frame

Design loads for the pendulum mass lifting frame were determined from the structural analysis of the pendulum support frame as discussed above. As with the pendulum support frame, the critical loading condition is just before release, when the pendulum mass has been lifted to its required drop height (Figure 4.12).

FSEL has a set of general-purpose W-shape columns available for use on any project within the lab. It was decided that the most inexpensive and

37

expeditious design of the pendulum mass lifting frame would incorporate the use of one of these columns.

After conducting an elastic analysis of a single W-shape cantilever column as the pendulum mass lifting frame, it was evident that the capacity of the laboratory strong floor was insufficient to support the design loads. The solution to this problem was to support the column laterally in the swing direction using a steel pipe backstay fabricated from scrap steel at Ferguson Laboratory. The addition of the backstay transformed the structural system of the pendulum mass lifting frame to a vertical propped cantilever, easily modeled in MASTAN 2. As anticipated, the backstay dramatically increased the capacity of the pendulum mass lifting frame and also reduced its deflections.

4.6.2 Design of Electric Winch and Pulley System for Pendulum Mass Lifting Frame

The second challenge in the design of the pendulum mass lifting frame design was to develop a lifting mechanism for the pendulum mass. Initially, an electric winch was purchased and mounted to the top of the W-shape column. Initial lifting tests of the pendulum mass showed that when the cable wound onto the winch spool, it applied a load parallel to the web of the W-shape, at a varying eccentricity from the plane of the web, thereby applying a torque about the vertical axis of the W-shape. Due to the low torsional stiffness of this W-shape with unrestrained flanges, it experienced large torsional deformations, and it was decided to re-design the lifting scheme.

To eliminate the eccentricity of loading, a large pulley was fabricated and mounted at the top of the W-shape to keep the lifting cable in the plane of the web of the W-shape. The electric winch was then relocated to the bottom of the W-shape, where any eccentricity of load produced as the lifting cable wound back

and forth on the spool could easily be transferred to the fixed base of the lab strong floor. The final result was a safe and reliable means of lifting the pendulum mass prior to each pendulum impact test.

4.7 CONCLUDING REMARKS REGARDING THE DESIGN OF THE IMPACT TEST PENDULUM

The impact test pendulum at the UT was developed to simulate a NCHRP TL-3 vehicular impact against a bridge barrier. Much design effort to include criteria such structural performance, constructability and laboratory resources went into the development of every component of the setup. The final design meets all performance criteria, and is currently operational at Ferguson Laboratory.

A large amount time and physical effort went into the fabrication and erection of the pendulum support frame during the summer of 2004. The construction of the pendulum support frame was an excellent exercise in structural fabrication, construction logistics, project management and teamwork, and quite a bit was learned by all involved in the process. The efforts of undergraduate assistants and fellow Graduate Research Assistants were vital in accomplishing the large amount of work on an abbreviated schedule. Finally, much credit is also due to the Ferguson Laboratory technical staff for providing foresight and experience in areas where the author had little or none.

CHAPTER 5

Validation of Impact Test Pendulum

5.1   INTRODUCTION

Before Ferguson Laboratory's impact test pendulum could be used to investigate the impact performance of retrofit bridge barriers, it had to be shown capable of accurately simulating a crash test to TL-3 of *NCHRP Report 350*. To accomplish this objective, and also to design the crush package for the pendulum, UT Austin researchers conducted a series of pendulum impact tests against a rigid barrier. Instrumentation for the rigid-barrier impact tests includes a Motorola 250-g accelerometer (Model No. MMA1200D), and a National Instruments 96-channel Signal Conditioning Chassis (Model No. NI SCXI-1001).

Signals from the chassis were read using the Ferguson Laboratory's LabView-based data-acquisition program, converted from analog to digital format, stored in a Windows®-based microcomputer, and transferred to the Ferguson Laboratory's computer network for permanent storage and post-processing.

Using LabView and the Signal Conditioning Chassis, a data acquisition program was written to read voltage measurements from the accelerometer during the pendulum collision.

From data acquired from rigid-barrier impact tests, researchers at UT Austin were able to develop crush packages (for the nose of the pendulum) with adequate energy absorption and appropriate crushing characteristics. In addition, a systematic method for data acquisition and post-processing was developed so

that researchers could evaluate the performance of each crush-package design. Finally, data from rigid-barrier impact tests were compared with NCHRP TL-3 crash test data, using the following criteria:

o   impact energy of the impact test pendulum system;
o   acceleration-time history of the pendulum impact; and
o   impulse of pendulum impact.

By comparing the acceleration histories from NCHRP crash tests, pendulum impact tests, and LS-DYNA finite element analytical models, the experimental testing program of the impact test pendulum at UT Austin was validated.

5.2   BACKGROUND ON VALIDATION OF IMPACT PENDULUM

To ensure that the impact test pendulum satisfies *NCHRP Report 350* TL-3 test criteria, the pendulum must impart sufficient impact energy, and also must produce an acceleration history similar to that of an actual vehicular collision. If it satisfies those criteria, the pendulum is an acceptable "surrogate vehicle." *NCHRP Report 350* specifically states that a surrogate-vehicle test should be modeled to simulate the behavior of a specific production vehicle. Because significant research exists in the area of crash testing, determining the actual acceleration history for a specific TL-3 crash test is primarily a matter of literature research.

5.2.1   Typical Acceleration History from an NCHRP TL-3 Crash Test

For further study, UT Austin researchers selected impact acceleration data from an NCHRP TL-3 crash test conducted at the Texas Transportation Institute

41

(TTI) in August 2002. This test measured the behavior of a 1997 Geo Metro colliding with a TxDOT T77 steel bridge barrier (TTI 2002).

With those test data, UT Austin researchers compared rigid-barrier impact test acceleration histories of each crush package design against the specific crushing characteristics of a 1997 Geo Metro. When a reasonable agreement between the impact acceleration histories of the crush package and the 1997 Geo Metro was achieved, the impact test pendulum was judged capable of impacting a test barrier with a force-time impulse consistent with that of an actual vehicular crash test. Therefore, the impact-test pendulum could be considered an appropriate surrogate vehicle.

Figure 5.1(a) shows the history of transverse acceleration (normal to the plane of the longitudinal barrier) during the Geo Metro collision against a steel bridge barrier. Information in that history includes the following:

o   duration of the impact;
o   maximum acceleration of the impact;
o   acceleration history during the impact; and
o   impulse of the impact.

NCHRP TL-3 Impact Test Acceleration Profile

(a) (b)
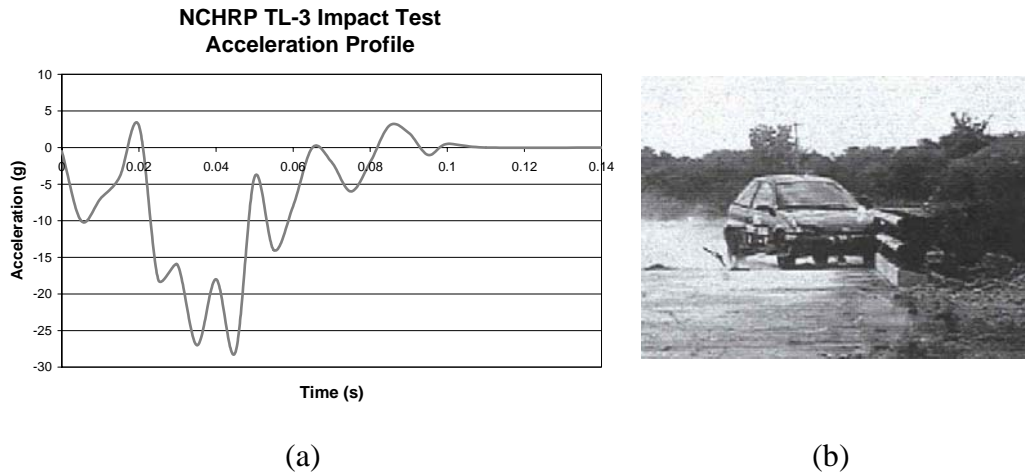
Figure 5.1- Geo Metro NCHRP TL-3 crash test (a) acceleration history and (b) photograph of impact with steel bridge barrier (TTI Research Report 4288-1)

To ensure that the impact test pendulum accurately simulates the acceleration history of a 1997 Geo Metro impact, all four of these factors must be taken into account when assessing the performance of a crush package design. The most important criterion, however, is that the force-time history of a pendulum test impact have an impulse similar to that of the 1997 Geo Metro impact.

5.2.2   Impulse Criterion for Vehicular Impact

Impulse is defined as change in momentum, or, if mass is conserved, mass multiplied by change in velocity. A simplified impulse-momentum equation (Equation 5-1) shows that the impulse of a collision can be calculated directly from the product of mass and an integrated acceleration history:

$$\text{Impulse} = \vec{I} = m \cdot \left(\vec{v}_o - \vec{v}_f \right) = \int_{t_o}^{t_f} \vec{P} \cdot dt = m \cdot \int_{t_o}^{t_f} \vec{a} \cdot dt \qquad (5\text{-}1)$$

43

Because of the physical relationship between impulse and acceleration, it is necessary to obtain reliable acceleration data from the pendulum impact tests. Acceleration histories are the primary means of comparing the results of a rigid barrier impact test and the acceleration history of the 1997 Geo Metro crash test.

5.3 PRELIMINARY DEVELOPMENT OF CRUSH PACKAGE

The development of a crush package that would simulate the specific crushing characteristics of a 1997 Geo Metro is a prerequisite to any meaningful testing of TxDOT bridge barriers. To accomplish this, the pendulum mass was tested against a rigid barrier consisting of a stiff steel buttress (Figure 5.2), and test impact accelerations were measured with an accelerometer mounted directly on the pendulum mass. The purpose of testing with a rigid barrier was to remove any possible deformation response of a bridge barrier from the pendulum impact acceleration history, thereby isolating the behavior of the crush package for examination and design refinement.

(a)   (b)
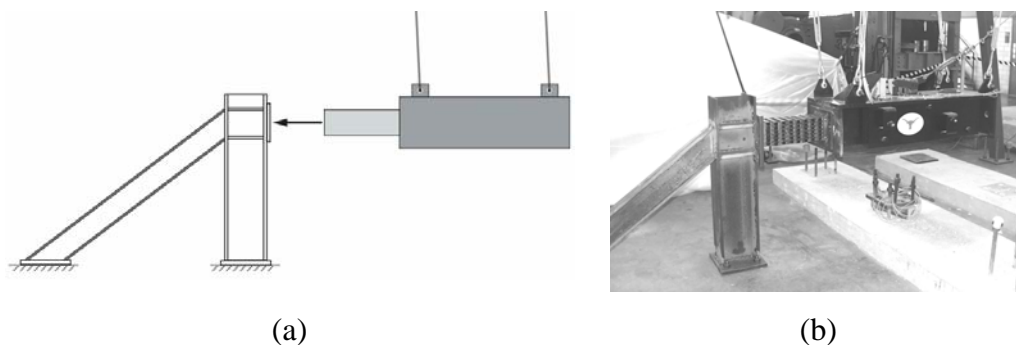
Figure 5.2(a) and (b)- Rigid barrier with pendulum mass and crush package

Initial development of the crush package involved the exploration of different materials and fabrication techniques. Using trial and error, crush

package designs were tested against the rigid barrier and evaluated based on energy absorption capacity and crushing characteristics. Design for the crush packages is discussed in the following sections.

5.3.1 Crush Packages of Autoclaved Aerated Concrete (AAC)

Figure 5.3 shows a rigid barrier impact test using a crush package of autoclaved aerated concrete (AAC), a lightweight cellular cementitious building material. Initially, AAC was considered for the crush package because it is inexpensive, has low strength, and is manufactured in convenient rectangular blocks.
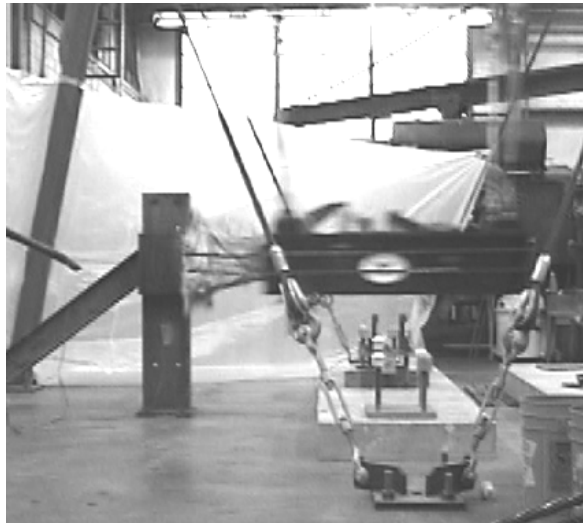
(a) impact

(b) after impact

Figure 5.3(a) and (b)- Rigid barrier impact of an AAC crush package

AAC, the first material tested as a crush package, was ultimately eliminated because did not absorb enough energy. Even without examining acceleration data, the large rebound of the pendulum mass from the rigid barrier, shown in Figure 5.3(b), indicates insufficient energy-absorption capacity.

Although the AAC was ultimately rejected for the crush package, its ease of use made it possible to test frequently, which lead to an expeditious development of a standard testing protocol, which was used for subsequent rigid-barrier impact tests.

5.3.2   Design of Tubular Steel Crush Packages

To increase its energy-absorption capacity, a decision was made to fabricate the crush package out of thin-walled square steel tubing ($1\times1\times0.049$-in., or $25.4\times25.4\times1.2$-mm), oriented so that the axes of the tubes would lie in planes normal to the impact direction of the pendulum mass. To identify an appropriate initial geometry for the crush package, force-deformation plots were obtained by crushing 6-in. (152.4-mm) prisms with various cross-sectional areas (Figure. 5.4).

6x6x6 in. Test Cube Load-Deformation Plot

(a)   (b)
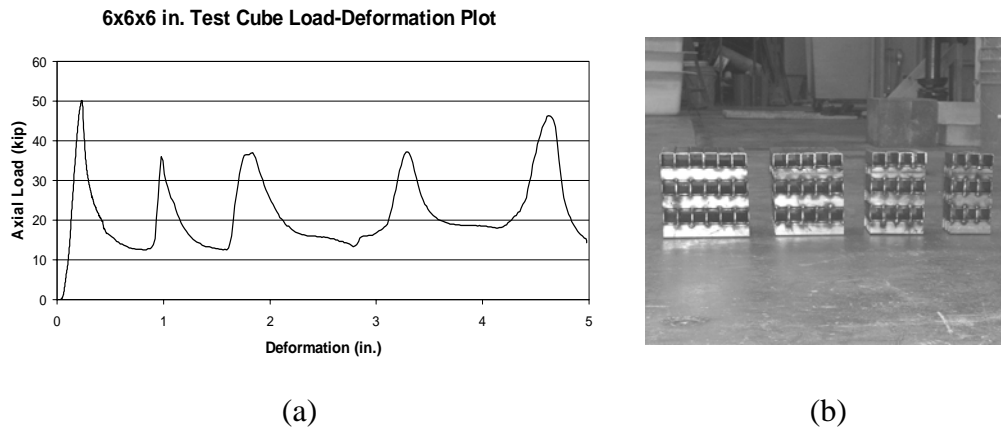
Figure. 5.4(a)- Force-deformation plot for a test prism, and (b) the various test prisms tested

Two characteristics of each test prism can be determined from its force-deformation plot: 1) the axial crushing capacity; and 2) the energy-absorption capacity. The axial crushing capacity is simply the maximum load obtained during crushing. The energy-absorption capacity is determined by integrating the force-deformation plots. The energy absorbed in crushing is divided by the number of layers in each test prism to determine the approximate energy absorption per layer. Using this methodology, the energy-absorption capacity of a crush package can be estimated as the sum of the energy-absorption capacities for each layer of the package.

These two characteristics –axial crushing capacity and energy-absorption capacity –can be used to establish trial designs for the crush package. For any particular tube geometry, axial crushing capacity is proportional to the cross-sectional area of the package, and energy-absorption capacity is proportional to the number of layers. The required cross-sectional area is based on the maximum

desired impact force, and the required energy-absorption capacity (*i.e.,* the required pendulum length) is based on the total impact energy of the test pendulum mass.

5.3.3   Development of First-Generation Tubular Steel Crush Package

Figure 5.5 shows the first tubular steel crush package tested against a rigid barrier. The crush package was fabricated by welding together individual 1-in. (25.4-mm) steel tubes into 6×6×1-in. (152×152×25-mm) layers, and then connecting those layers. Stiff bars, oriented parallel to the layers, were also welded to the outside of the crush package to prevent the layers from separating during impact. To be conservative, the nose was made longer than required to ensure enough energy-absorption capacity and to limit the impact force.
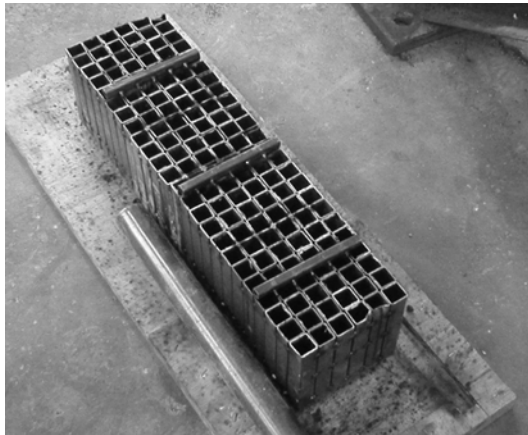
Figure 5.5- First-generation tubular steel crush package

Unfortunately, the first tubular steel crush package had stability problems. Figure 5.6 shows the pendulum test impact against the rigid barrier. The package did not crush in a controlled, regular manner, and although it had enough layers of steel tubes to stop the pendulum, the pendulum yawed severely on impact.
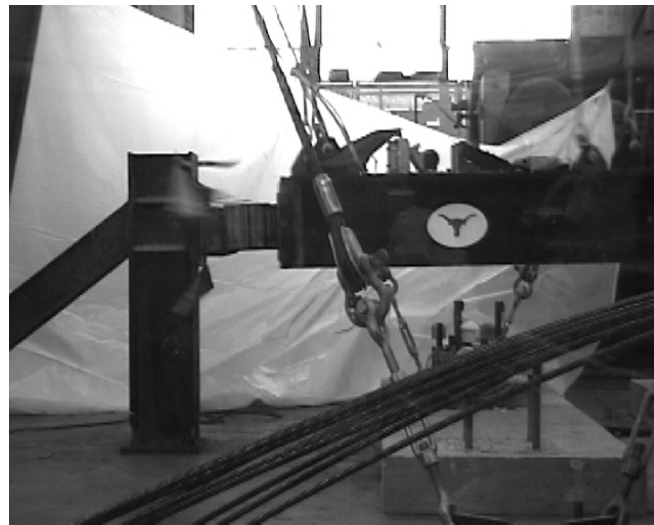
(a) impact
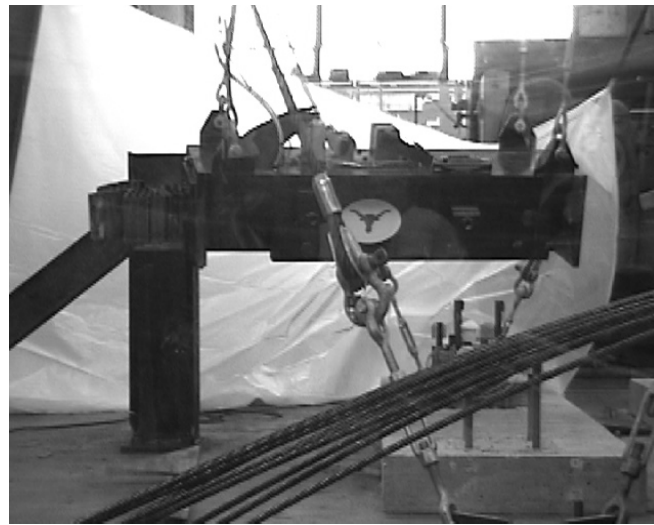
(b) after impact

Figure 5.6(a) and (b)- Rigid-barrier impact test of first-generation steel crush package

51

The unstable crushing of the first-generation steel crush package made it an unacceptable design. After a post-test analysis of this crush package design, the source of the instability became apparent, and is illustrated in Figure 5.7.

(a)   (b)
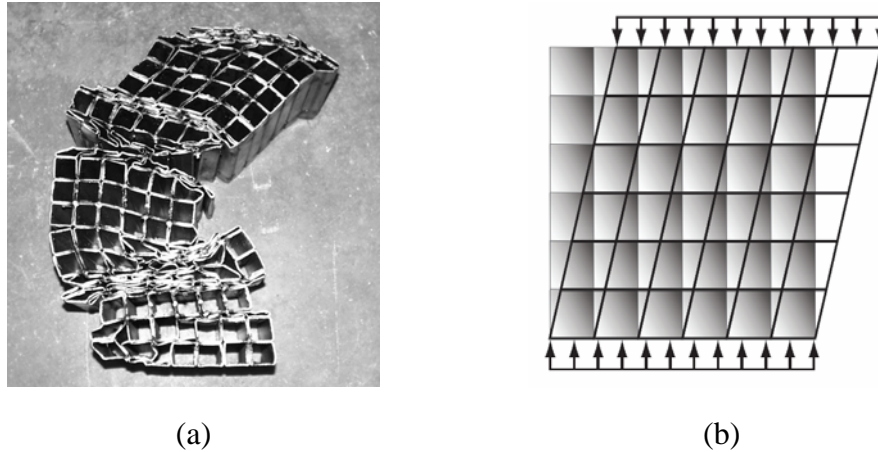
Figure 5.7(a)- Post-test condition and (b) planar failure mechanism for the first- generation steel crush package

The instability of the first-generation crush package during a pendulum test impact can be considered analogous to that of a planar, unbraced frame (Figure 5.7), collapsing laterally due to accumulated story drifts in the same direction.

5.3.4   Development of Second-Generation Tubular Steel Crush Package

Using the multi-story frame analogy, the decision was made to "brace" adjacent layers of the crush package by orienting the tubes in adjacent layers in

52

criss-cross fashion (changing the axes of the tubes by 90 degrees from layer to layer), as shown in Figure 5.8.

Figure 5.8- Second-generation tubular steel crush package

In addition to being more stable laterally, the second-generation steel crush package was also easier to fabricate. The multi-directional arrangement of tubes facilitates a more consistent welding scheme along the outside of the crush package, and also eliminates the need for the stiff bracing rods required in the first-generation steel crush package.

The crushing behavior of the second-generation steel crush package is shown in the pendulum test impact photographs in Figure 5.9(a) and (b). The second-generation steel crush package had sufficient energy-absorption capacity to stop the pendulum, and its crushing behavior was controlled and stable throughout impact. After the test, close inspection of the crush package confirmed the predicted crushing mechanism (Figure 5.10).

(a) impact
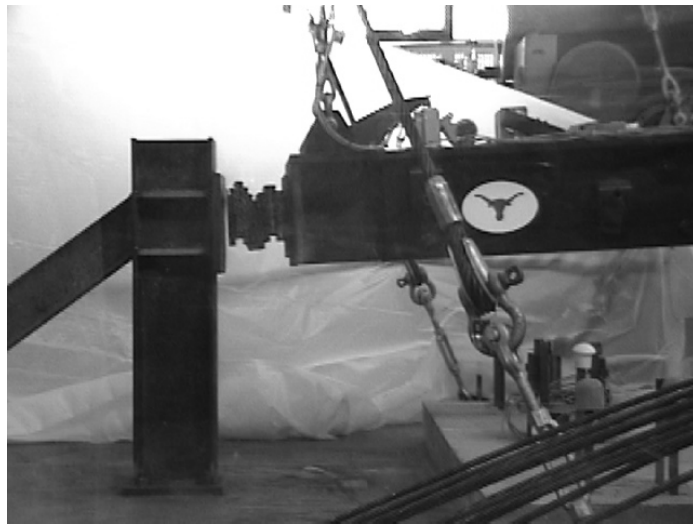
(b) after impact

Figure 5.9(a) and (b)- Rigid barrier impact test of a second-generation steel crush package

(a)   (b)
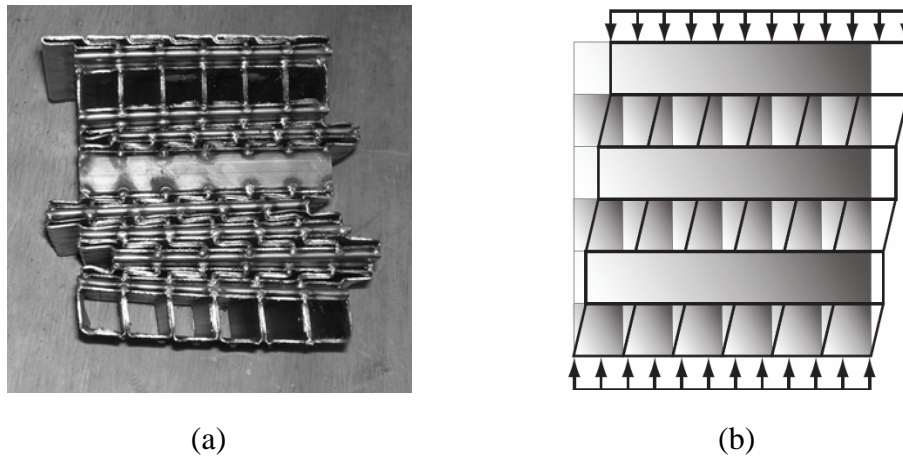
Figure 5.10(a)- Post-test condition of the second-generation steel crush package and (b) failure mechanism

The improved crushing performance of the second-generation crush package was due to its increased lateral stability under impact loads. By alternating the orientations of the tubes in adjacent layers, sway of all layers in the same direction was precluded, and the package was forced to crush essentially axially (Figure 5.10).

Additionally, some layers in the second-generation steel crush package did not crush, showing that the package has more than enough energy-absorption capacity. Multiple tests confirmed that the second-generation crush package always had about 2 or 3 uncrushed layers after each test, indicating consistent energy-absorption characteristics from test to test.

5.3.5   Conclusions regarding Behavior of Steel Tube Crush Package

The above observations clearly indicate that the second-generation steel crush package behaves better than other designs considered by UT Austin researchers. It was decided to use this type of crush package for subsequent impact tests.

5.4 INITIAL REMARKS REGARDING ACQUISITION AND POST-PROCESSING OF ACCELERATION DATA FROM PENDULUM TESTING

Acceleration histories for each crush package were acquired from an accelerometer mounted directly to the pendulum mass, and a high-speed data acquisition system that samples data points at 5000 Hz during a pendulum impact test. No other instrumentation was required for the rigid-barrier impact tests.

The acceleration history from each rigid-barrier impact test was used to compare the performance of each crush-package design with the acceleration history of the 1997 Geo Metro crash test. Because acceleration data are so critical to Project 0-4823, UT Austin researchers needed to develop a systematic way to acquire and process those data, as outlined in this section.

During a pendulum test impact, the accelerometer mounted on the pendulum mass does not discriminate between accelerations generated from the pendulum impact with the rigid barrier, and accelerations associated with subsequent axial vibrations of the pendulum mass induced by that impact. The result is raw accelerometer data that contain more information than necessary or desirable to determine the acceleration history for each crush package. Although the impact acceleration history of the crush package is embedded within those raw data, high-frequency axial vibration of the pendulum mass obscures that history, and must be removed using digital post-processing.

Initial observations from low-energy impact tests of the pendulum mass against the rigid barrier indicated that the characteristic frequencies of axial vibration of the pendulum mass were much higher than those associated with the primary impact. It was therefore concluded that the axial vibrations of the pendulum mass could be filtered from the raw accelerometer data using a low-pass filter (one that would allow low frequencies to pass, while removing high frequencies).

56

5.5 DESIGN OF LOW-PASS FILTER FOR PROCESSING DATA FROM RIGID-BARRIER IMPACT TESTS

Because no explicit guidelines exist for designing an appropriate low-pass filter for the raw accelerometer data, it was designed by trial and error, using the *Signal Processing Toolbox* of Matlab 6 (MathWorks 2002). This program contains a platform to which the raw accelerometer data can be imported, and also provides a graphical user interface for designing and applying various filtering algorithms. The filtering algorithm selected was a Butterworth low-pass filter, whose filtering characteristics are shown in Figure 5.11.

Butterworth IIR Low-Pass Filter
(120 Hz Corner Frequency)
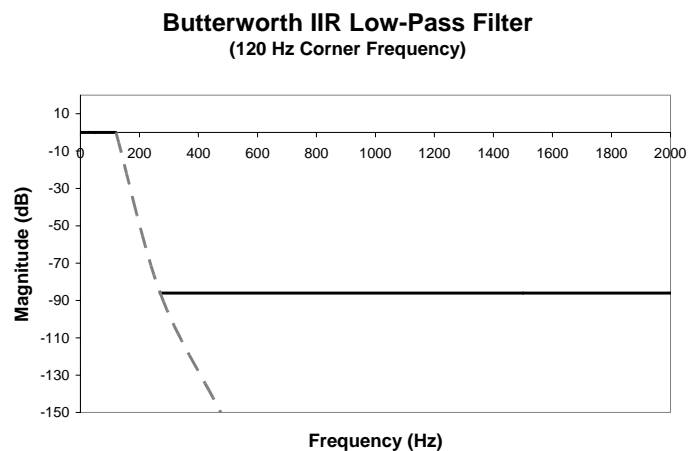
Figure 5.11- Frequency characteristics of Butterworth low-pass filter

The filter has three characteristics: 1) a low-frequency range in which data pass through; 2) a transition range; and 3) a high-frequency range in which data are greatly attenuated. The frequency at the low end of the transition range, known as the "corner frequency," is shown as 120 Hz in Figure 5.11.

The corner frequency separates the frequencies of raw data that are permitted to pass through, from those that are filtered. The final value of the corner frequency was determined by running the raw accelerometer data through

several trial low-pass filters, each with a different corner frequency, and observing the sensitivity of the filtered data to the value of the corner frequency.

5.5.1   Effects of Corner Frequency of Low-Pass Filter

Figure 5.12(a) and (b) respectively show the sensitivity of the impulse value and the maximum acceleration value of an impact acceleration history dataset to changes in the corner frequency. While Figure 5.12(a) shows that impact impulse is relatively insensitive to corner frequencies above about 100 Hz Figure 5.12(b) shows that maximum acceleration values generally decrease as the corner frequency is reduced.

Impulse vs Corner Frequency
(Crush Package #2 Dataset)

(a)

Max Acceleration vs Corner Frequency
(Crush Package #2 Dataset)
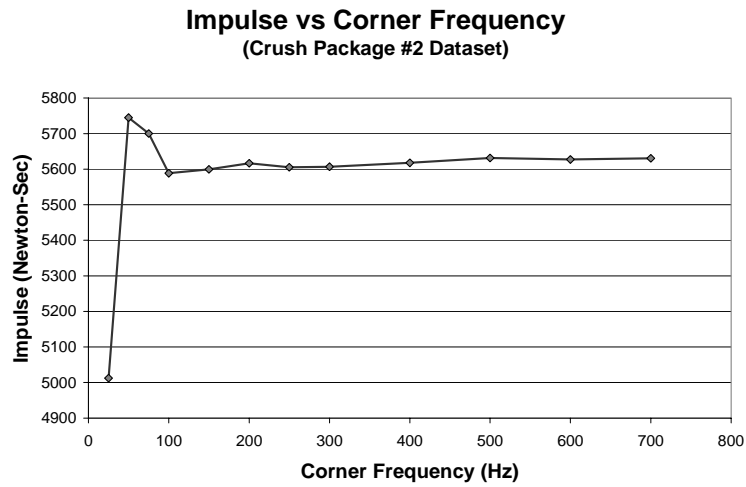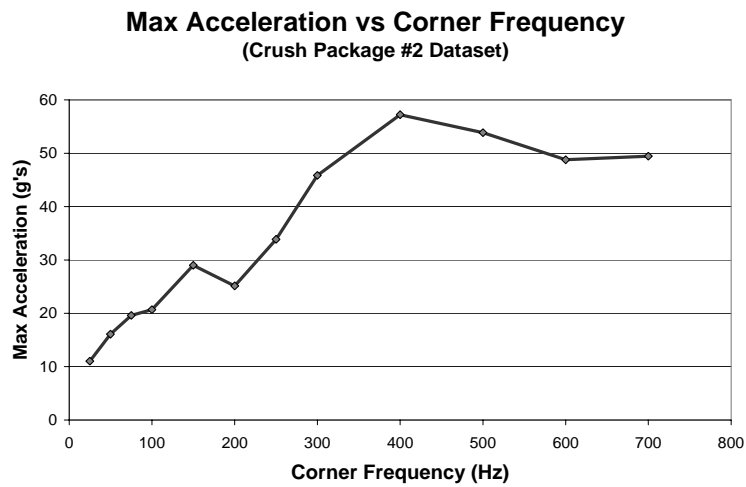
(b)

Figure 5.12(a)- Impulse values of the accelerometer signal and (b) maximum
acceleration values as a function of low-pass filter corner frequency

59

Because impulse is the primary criterion for evaluating the performance of a crush package, and, as shown in Figure 5.12(a), the impulse value is constant through a large range of corner frequency values, it was decided to use Figure 5.12(a) as the primary criterion in determining a suitable corner frequency for the Butterworth low-pass filter.

The final value of 120 Hz for the corner frequency was determined by observing that it preserved the impulse, and reasonably preserved the maximum acceleration. For data from several rigid-barrier pendulum tests, the selected corner frequency of 120 Hz consistently produced filtered data with impulse values in the plateau range of Figure 5.12(a), and maximum acceleration values similar to those of the Geo Metro crash test.

While preserving impulse and maximum acceleration values, low-pass filtering with a corner frequency of 120 Hz filtered out most of the extraneous high-frequency response of the pendulum mass itself, making the overall data history much easier to interpret (Figure 5.13).

Unfiltered Acceleration Profile
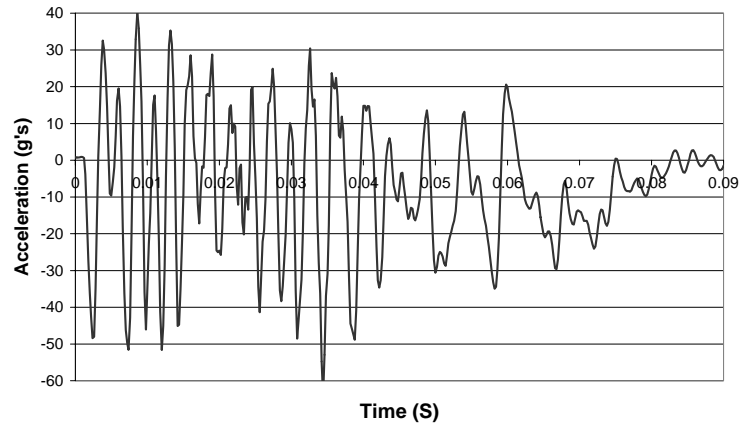
(a)

120 Hz Filtered Accleration Profile
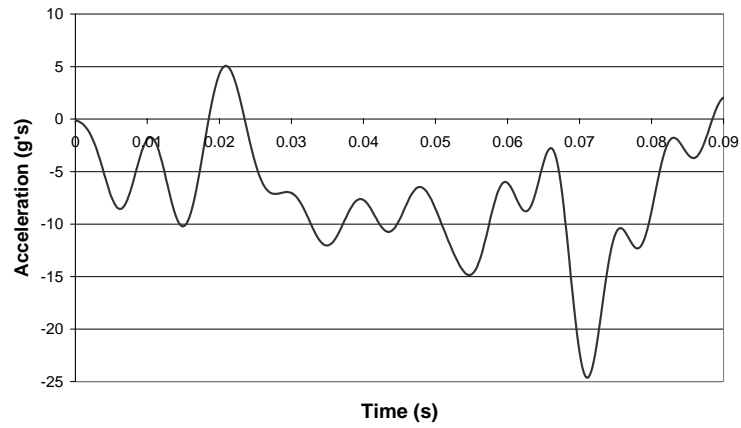
(b)

Figure 5.13-(a) Unfiltered acceleration history from a pendulum impact test,
and that data filtered at (b) 120Hz

61

5.6 FURTHER EVALUATION OF RESULTS FROM RIGID-BARRIER IMPACT TESTING USING FILTERED ACCELERATION DATA

As discussed in Section 5.3, several rigid-barrier impact tests were conducted to refine the material and geometric properties of the crush package. Observations from these tests suggested that the second-generation steel crush package design be used as a starting point for crush package development.

Using the techniques just described for the post-processing of acceleration data, UT Austin researchers continued development of the crush package. The impact acceleration history corresponding to each crush package was compared to the acceleration history of the 1997 Geo Metro crash test, and also to that produced using analytical simulations of the pendulum and Geo Metro tests, as discussed in Tolnai (2005). These comparisons are presented and discussed in the following subsections.

5.6.1 Performance of Second-Generation Crush Package #1

Figure 5.14(a) and (b) show, respectively, a dimensional schematic and photograph of second-generation Crush Package #1 (the "second-generation" crush package whose initial development is discussed in Section 5.3.4 It has a uniform cross-sectional area of 36 in.^{2} (232 cm^2) and a length of 18 in. (457 mm).
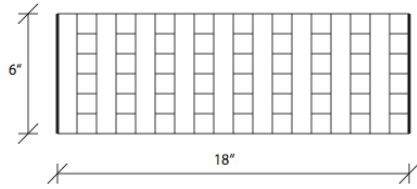
(a)	(b)

Figure 5.14(a) and (b)- Second-generation Crush Package #1

The acceleration history of this crush package design is compared to that of the Geo Metro crash test in Figure 5.15(a). While the impact duration and maximum acceleration are similar to the Geo Metro crash, but the overall shape of the acceleration history for Crush Package #1 does not match well. Similar impact durations (within 0.015 s) suggest that Crush Package #1 is long enough, and similar maximum accelerations indicate that its cross-sectional area is reasonable.
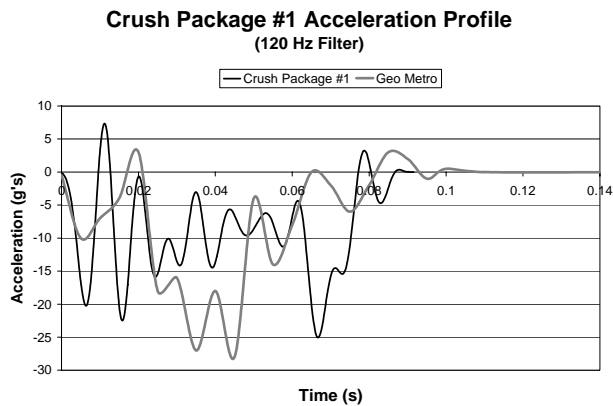
(a)	(b)

Figure 5.15(a)- Acceleration history of crush package #1 and (b) photo of test

High accelerations at the start of the pendulum impact (0.00-0.02 s), however, suggest that the impact force is too high then. This suggests that, although a cross-sectional area of 36 in.^{2} (232 cm^2) is appropriate for the maximum acceleration value of the impact, the cross-sectional area at the front of Crush Package #1 should be reduced, so that the resulting force history would more closely match the acceleration history of the Geo Metro crash test.

Finally, the acceleration history of Crush Package #1 has an impulse of 6625 N-seconds, within 5% of the impulse value of the Geo Metro impact (6846 N-sec). This is good agreement.

In summary, the performance of Crush Package #1 can be described as follows, compared to the Geo Metro crash test:

o   good agreement in impact duration;

o   good agreement in peak acceleration;

o   poor agreement of acceleration history; and

o   good agreement in impulse.

5.6.2   Performance of Second-Generation Crush Package #2

Using the above observations of the performance of Crush Package #1, Crush Package #2 was designed using a non-uniform cross-section, in an attempt to more closely match the Geo Metro acceleration history. Figure 5.16 shows the non-uniform cross-section of Crush Package #2.

<center>(a)   (b)</center>
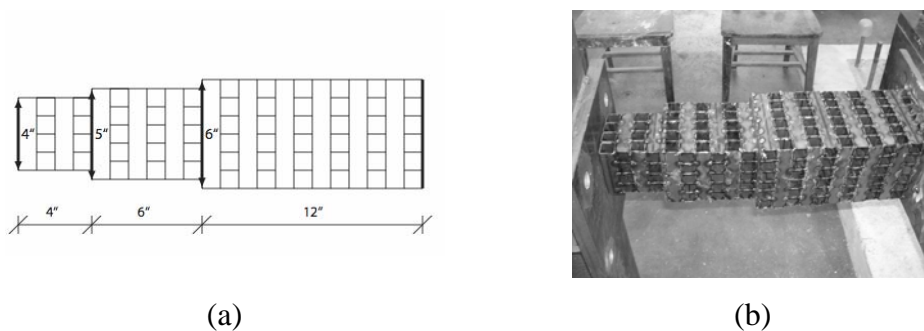
Figure 5.16(a) and (b)- Second-generation Crush Package #2

In Figure 5.17, the acceleration history using Crush Package #2 is compared to that of the Geo Metro crash test. The acceleration history from Crush Package #2 follows the history for the Geo Metro impact much more closely, than did the history from Crush Package #1. The peak acceleration for Crush Package #2 is the same as for Crush Package #1 (and for the Geo Metro), at about 25 g. This is expected because both crush packages have the same cross-sectional area of 36 in.^{2} (232 cm^2). Nevertheless, some differences still exist between the acceleration history from Crush Package #2, and from the Geo Metro. The peak acceleration from the crush package occurs at 0.07 sec, while the peak for the Geo Metro occurs at about 0.05 sec.

<center>65</center>

Crush Package #2 Acceleration Profile
(120 Hz Filter)
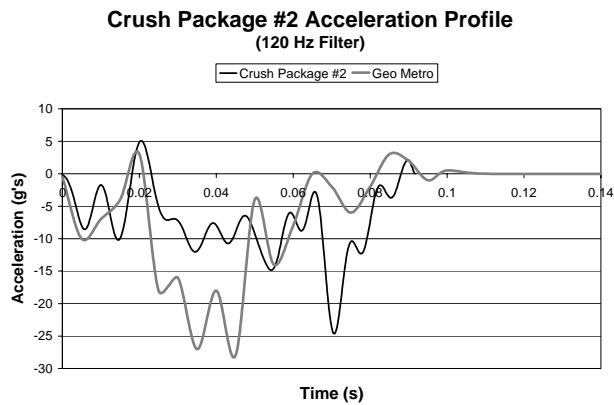
(a)   (b)

Figure 5.17(a)- Acceleration history for Crush Package #2 and (b) photo of test

Because the cross-sectional area of Crush Package #2 is non-uniform, its acceleration history shows when each separate cross-section begins to crush. Figure 5.18(a) shows the acceleration history of Crush Package #2 with the approximate time of impact of each cross-section. Figure 5.18(b) shows a schematic of Crush Package #2 with the times of impact labeled at the appropriate locations along its length.

Crush Package #2 Acceleration Profile

(a)   (b)
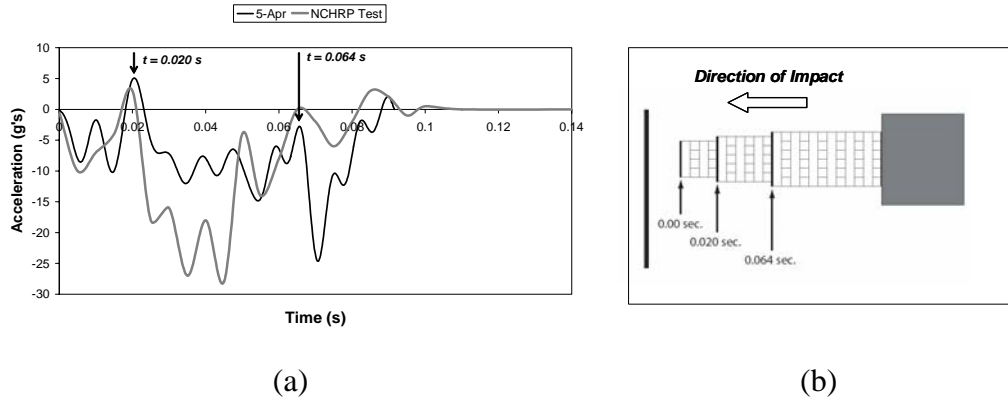
Figure 5.18(a)- Acceleration history for Crush Package #2 and (b) time of impact for each cross-section of Crush Package #2

As the crush package impacts the rigid barrier, the accelerations in Figure 5.18(a) increase with increasing cross-sectional area of the crush package in Figure 5.18(b). For the first two cross-sections of the crush package, the length of each cross-section is proportional to its crushing duration in Figure 5.18(a).

This is not the case, however, for the third cross-section of Crush Package #2. The reason for this apparent discrepancy is shown in the impact test video. During the crushing of the third cross-section, many layers of the crush package crush simultaneously, and some layers don't crush at all.

Finally, the calculated impulse from Crush Package #2 is 5581 N-sec, within 20% of the impulse from the Geo Metro crash test. This agreement was judged acceptable.

67

In summary, the performance of Crush Package #2 can be described as follows, compared to the Geo Metro crash test:

o   good agreement in impact duration;

o   good agreement in peak acceleration;

o   much better agreement acceleration history; and

o   acceptable agreement in impulse.

Based on the acceleration history of Crush Package #2, researchers at UT Austin learned how to predict the behavior of a crush package based on the cross-sectional area and the lengths of its component sections.

5.6.3   Performance of LS-DYNA Analytical Model

Figure 5.19(a) compares the acceleration history from an LS-DYNA simulation (Tolnai 2005) with the acceleration history from the Geo Metro crash test. The LS-DYNA history does not match the duration or shape of the Geo Metro history. Nevertheless, it does match the peak acceleration within 30% and, at 7274 N-sec, matches the impulse within 10 %.

DYNA Acceleration Profiles

(a)

(b)

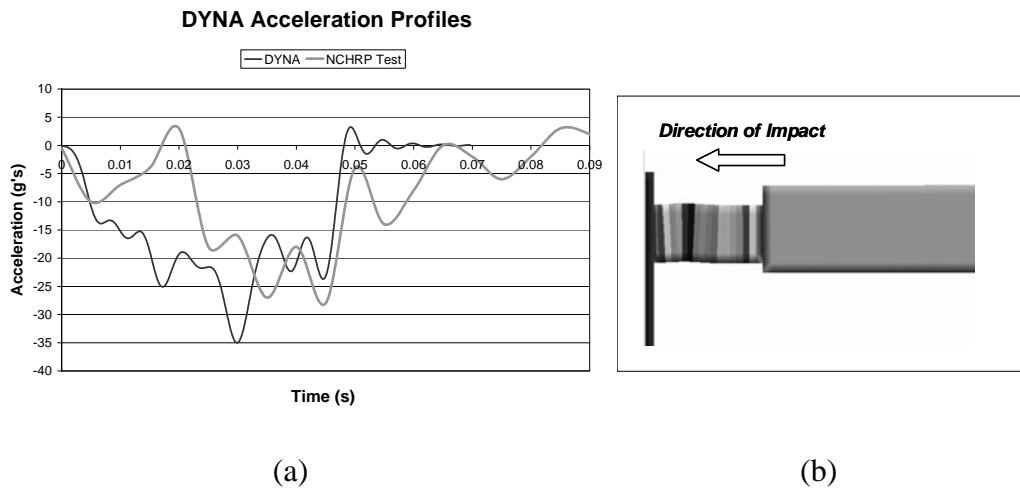*Figure 5.19(a)- Acceleration history from LS-DYNA simulation and (b) screen shot of the computer simulation (Tolnai 2005)*

Although the LS-DYNA output does not match all aspects of the all of the Geo Metro impact acceleration history criteria, it does match the impulse quite well, suggesting that LS-DYNA is a valuable tool for the validation of the impact test pendulum at UT Austin. This is discussed further in Tolnai (2005).

5.6.4 Significance of Results for Validation of Impact Test Pendulum

Figure 5.20 is a graphical comparison of the impact impulses of the two pendulum tests (Crush Package #1 and #2, the NCHRP Geo Metro test, the LS-DYNA simulation, and the theoretical impulse, calculated using Equation 5-1.

Impulse Comparisons

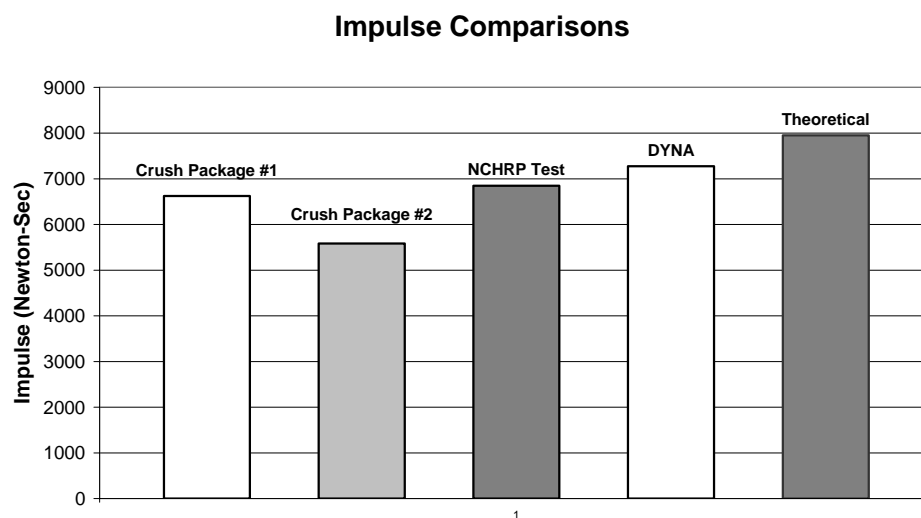*Figure 5.20- Comparison of impulse levels among impact tests*

Both pendulum tests and the LS-DYNA simulation acceptably match the impact impulse of the Geo Metro. Because impact impulse is the primary criterion for the bridge barrier testing program of Project 0-4823, Figure 5.20 suggests that the impact test pendulum and the LS-DYNA analytical model are reasonable methods of simulating an NCHRP TL-3 vehicular impact.

70

5.7 CONCLUDING REMARKS REGARDING VALIDATION OF IMPACT TEST PENDULUM

The goal of the researchers at UT Austin is to simulate a NCHRP TL-3 vehicular impact with the impact test pendulum, using the acceleration history of a 1997 Geo Metro crash test as a benchmark. Rigid barrier impact tests were used to develop the crush package design and establish a data acquisition and post-processing methodology.

Various crush package designs were tested and compared against the Geo Metro acceleration history. Force levels were controlled by the cross-sectional area of the crush package, and impact duration by the lengths of the different components comprising the package.

Based on a comparison of impact impulses from the acceleration histories of the second-generation steel crush packages, the LS-DYNA analytical model, and a real Geo Metro test, it was concluded that the impact test pendulum and LS-DYNA analytical model can give good simulations of an NCHRP TL-3 vehicular impact.

CHAPTER 6

Summary, Conclusions, and Recommendations

6.1   SUMMARY

The purpose of Research Project 0-4823 ("*Performance Testing of Anchors for Retrofitting and Repair of Bridge Barriers"*) is to find out how to replace a standard TxDOT bridge barrier after the original has been damaged by a vehicular collision. The goal of Project 0-4823 is to determine how mechanical anchors can be used with retrofit TxDOT barrier designs that can perform like the corresponding cast-in-place bridge barriers.

To understand how a standard cast-in-place T203 bridge barrier behaves during a vehicular impact, an impact test pendulum was developed, and also a T203 bridge deck and barrier test specimen. Details are given in Chapter 3. The impact test pendulum currently serves as valuable tool for simulating the vehicular impact of a crash test to TL-3 (Test Level 3) of *NCHRP Report 350*, and details of its design and operation are presented in Chapter 4.

To validate the impact test pendulum, data from it were compared with results from the crash test of a 1997 Geo Metro and finite element analytical models using LS-DYNA, a widely used software package.

6.2 CONCLUSIONS

1) The impact test pendulum at Ferguson Laboratory successfully generates and delivers the impact energy required to meet *NCHRP Report 350* TL-3 testing criteria for bridge barriers, in a safe, predictable and consistent manner.

2) Pendulum-test video data and acceleration histories clearly show that the second-generation crush package, whose development is described in Section 5.3.4, can simulate TL-3 vehicular impacts. Although the detailed acceleration history does not always match that of the Geo Metro, the impact duration, maximum acceleration, and impulse agree well and satisfy *NCHRP Report 350* requirements.

6.3 RECOMMENDATIONS FOR FUTURE RESEARCH

Based on the research conducted by the author, the second-generation crush package needs additional refinement to match the detailed force-time histories of crash-test data. Current UT Austin research in this area focuses on the use of a variable cross-section to change the crushing characteristics along the length of the package.

APPENDIX A

A.1   CAST-IN-PLACE ANCHORS

Cast-in-place anchors are placed in position before concrete is cast. A cast-in-place anchor can be a headed bolt of standard structural steel, placed with its head in the concrete. It can also be a standard threaded rod and a hexagonal nut, with the nut end embedded in concrete. Finally, it can be a bar bent at one end and threaded at the other end, with the bent end placed in concrete. Figure A.1 shows these variations.
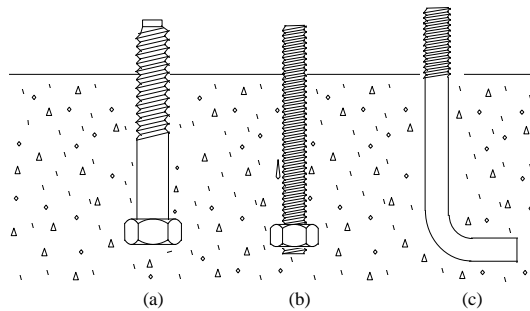

Figure A.1- Cast-in-place anchors

A headed cast-in-place anchor depends on mechanical interlock at the bolt head for load transfer. Some bond may also exist between the anchor shank and surrounding concrete.

A.2   POST-INSTALLED ANCHORS

Post-installed anchors are installed in existing concrete or masonry structures. They are widely used in repair and strengthening work, as well as in new construction, due to advances in drilling technology, and to the flexibility of installation that they offer. There are many different types of post-installed

74

anchors, classified according to their load-transfer mechanisms. The most basic distinction is between mechanical anchors and adhesive (or bonded) anchors. Because the scope of Research Project 0-4823 involves only the use of mechanical anchors, bonded anchors will not be mentioned further.

A.2.1   Mechanical Anchors

A.2.1.1 Expansion Anchors

An expansion anchor consists of an anchor shank with a conical wedge and expansion element at the bottom end (Figure A.2). The spreading element is expanded by the conical wedge during installation and throughout the life of the anchor. The spreading element is forced against the concrete wall of the hole as the wedge is pulled by tension on the anchor shank. The external load is transferred by the frictional resistance from the conical wedge to the spreading element, and from the spreading element to the surrounding concrete.
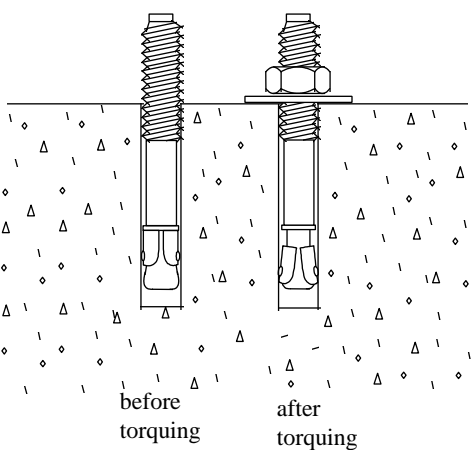

before
torquing

after
torquing

Figure A.2- Expansion anchors

Depending on the relative diameters of the bolt and the drilled hole, expansion anchors are classified as either bolt-type or sleeve-type anchors. For a

bolt-type anchor, the nominal diameter of the drilled hole equals that of the anchor bolt. For a sleeve-type anchor, the nominal diameter of hole equals that of the sleeve encasing the bolt. A wedge anchor is the most common bolt-type anchor.

A.2.1.2   Undercut Anchors

An undercut anchor is installed in a hole in the base material that is locally widened (undercut). The undercut hole accommodates the expansion elements of the anchor, expanded during installation. Undercut anchors mainly rely on bearing to transfer tension load.

Different undercut geometries are used for various undercut anchor systems. Figure A.3 shows the two different geometries of undercut anchors tested recently at UT Austin: Undercut Anchor 1 and Undercut Anchor 2, designated as UC1 and UC2 respectively. It can be seen from that figure that Anchor UC2 has a much smaller bearing area on the surrounding concrete than Anchor UC1.
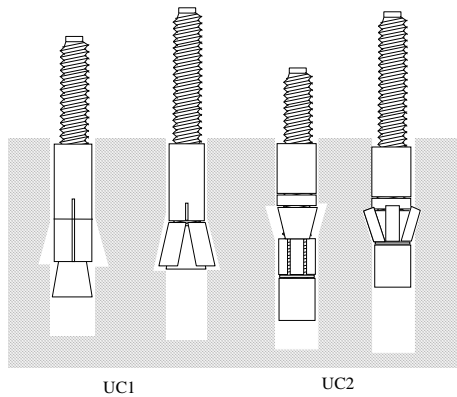
UC1   UC2

Figure A.3- Undercut anchors

A.2.2   Definitions of Embedment Depth

Anchors are commonly identified by a nominal embedment depth, used primarily to indicate the required hole depth. For most anchors, that nominal embedment depth is the length of the anchor. For cast-in-place anchors, it is the depth to the bearing surface. Nominal embedment depths are illustrated in Figure A.4(a).

The effective embedment depth of an anchor is the distance between the concrete surface and the bearing portion of the anchor head. For most anchors, the effective and nominal embedment depths are equal. Exceptions to this are some types of expansion anchors, whose contact point (a dimple on the clip) is considerably above the end of the anchor. Effective embedment depths are defined as shown in Figure A.4(b).For adhesive anchors, effective and nominal embedment depths are equal.
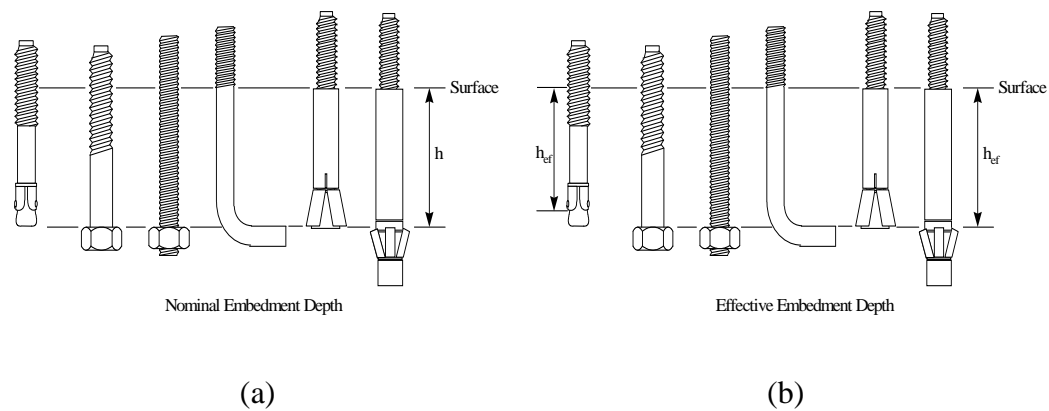
(a)   *(b)*

Figure A.4- Definitions of anchor embedment depths

A.2.3   Tensile Failure Modes

Depending on the type of anchor, the strength of the anchor steel, the strength of the surrounding concrete embedment, and sometimes also on the condition of the drilled hole during installation, a tensile anchor can exhibit different failure modes, each with a corresponding failure capacity. The following section explains all the failure modes of anchors in tension and the corresponding calculation procedures, if available.

A.2.3.1   Steel Failure in Tension

Steel failure occurs by yield and fracture of the steel shank of the anchor as shown in Figure A.5. The maximum fracture capacity of the anchor shank can be simply calculated from the effective tensile stress area of the anchor and the tensile strength of the anchor steel:

$$N_{sa} = nA_{se}f_{uta} \qquad \textbf{\textit{(A-1)}}$$

78

where: N_{sa} = tensile strength of a single anchor or group of anchors;

n = the number of anchors in the group;

A_{se} = effective tensile stress area of the anchor; and

f_{uta} = ultimate tensile strength of anchor steel.

When a threaded connection is involved, the effective tensile stress area should include the effect of the threads:

$$A_{se} = \frac{\pi}{4}\left[d_o - \frac{0.9743}{n_t}\right]^2 \quad (A\text{-}2)$$

where: d_o = the major diameter of the threaded part, inch; and

n_t = the number of threads per inch.

In practical terms, the effective tensile stress area is usually about 70% of the nominal (gross) area. Steel failure can also occur by thread stripping, if a shank at the lower limit of allowable tolerance is combined with a nut at the upper limit of allowable tolerance.
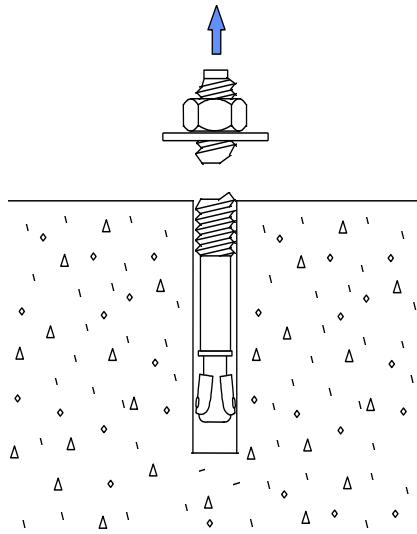
Figure A.5-Anchor steel failure under tensile load

A.2.3.2 Concrete Cone Breakout in Tension

Concrete breakout failure occurs by the propagation of a roughly conical fracture surface from the bearing edge of the anchor head of a cast-in-place anchor, or from the tip of the expansion mechanism of an expansion or an undercut anchor. The angle of the cone (α in Figure A.6), as measured from the concrete surface, increases from around 35° at shallow embedments, to about 45° at deep embedments.
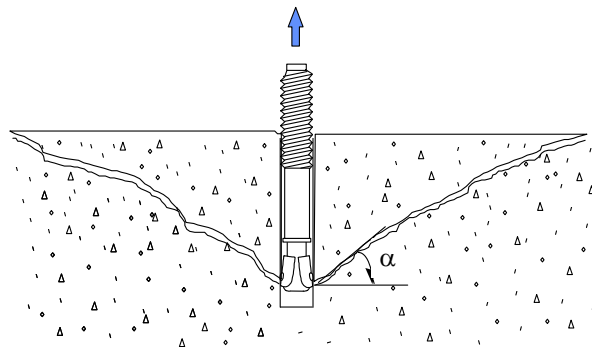

Figure A.6- Concrete breakout failure

The primary factors determining the concrete breakout capacity are the anchor embedment depth and the concrete strength. The most commonly accepted approach for predicting concrete capacity is the CC Method, which is the default approach of ACI 318-05 Appendix D.

A.2.4 Concrete Capacity Method (CC Method)

The CC Method, based on a large amount of test results and to some extent on fracture mechanics (Eligehausen and Sawade 1989), computes the concrete breakout capacity of a single tensile anchor far from edges as:

$$N_b = k_c \sqrt{f'_c} h_{ef}^{1.5} \qquad \textit{(A-3)}$$

where: N_b = tension cone breakout capacity;

k_c = constant; 24 for cast-in anchors, and 17 for post-installed anchors ;

f'_c = specified concrete compressive strength (6×12 cylinder) (inch in US units, MPa in SI units.); and

h_{ef} = effective embedment depth (inch in US unit, MPa in SI units).

In the CC Method, the breakout body is idealized as a pyramid with an inclination of about 35 degrees between the failure surface and the concrete member surface (Figure A.7). As a result, the base of the pyramid measures $3h_{ef}$ by $3h_{ef}$.
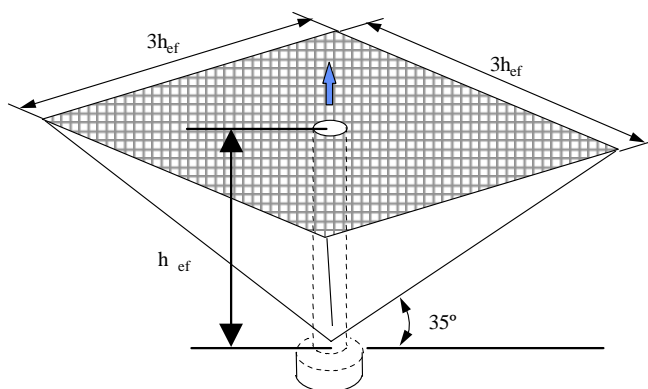

Figure A.7-Concrete tensile breakout body as idealized in CC Method

If the failure pyramid is affected by edges or by other concrete pyramids, the concrete capacity is calculated according the following equation:

$$N_{cb} = \frac{A_{Nc}}{A_{Nco}} \psi_{ed,N} \psi_{c,N} \psi_{cp,N} N_b \qquad (A\text{-}4)$$

where: A_{Nco} = projected area of a single anchor at the concrete surface without edge influences or adjacent-anchor effects, idealizing the failure cone as a pyramid with a base length of $s_{cr} = 3h_{ef}$ ($A_{Nco} = 9\ h_{ef}^2$);

A_{Nc} = actual projected area at the concrete surface;

$\psi_{ed,N}$ = tuning factor to consider disturbance of the radially symmetric stress distribution caused by an edge,

$\qquad$ = 1, if $c_{a,min} \geq 1.5h_{ef}$;

$\qquad$ = $0.7 + 0.3\dfrac{c_{a,min}}{1.5h_{ef}}$, if $c_{a,min} \leq 1.5h_{ef}$;

$\qquad$ where:

$\qquad\qquad$ $c_{a,min}$ = minimum edge distance to the nearest edge;

$\psi_{c,N}$ = constant; 1.25 for cast-in anchors, and 1.4 for post-installed anchors, where the value of k_c is 17;

$\psi_{cp,N}$ = modification factor for post-installed anchors designed for uncracked concrete without supplementary reinforcement to control splitting,

$\qquad$ = 1, if $c_{a,min} \geq c_{ac}$;

$\qquad$ = $\dfrac{c_{a,min}}{c_{ac}} \geq \dfrac{1.5h_{ef}}{c_{ac}}$, if $c_{a,min} < c_{ac}$;

$\qquad$ where:

$\qquad\qquad$ c_{ac} = 2.5h_{ef} for undercut anchors, 4h_{ef} for torque-controlled anchors, 4h_{ef} for displacement-controlled anchors;

A.2.5 Concluding Remarks

Using these design approaches, researchers at UT Austin will be able to design retrofit bridge barrier connections and predict the behavior of mechanical anchors subjected tensile loads produced by a vehicular impact.

APPENDIX B

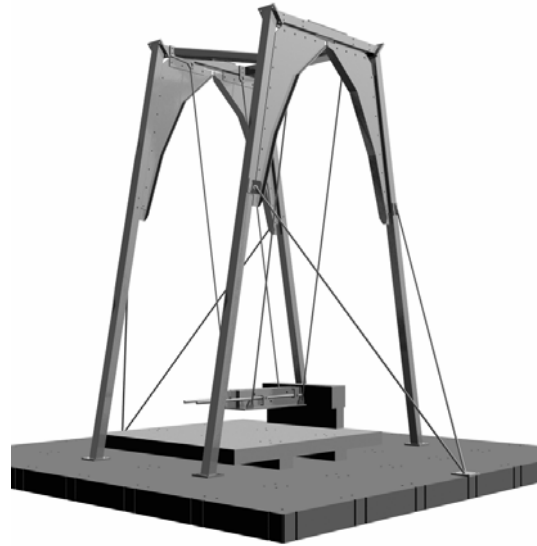## B.1   DESIGN MODELS FOR PENDULUM SUPPORT FRAME

Figure B-1- Isometric rendering of impact test pendulum setup

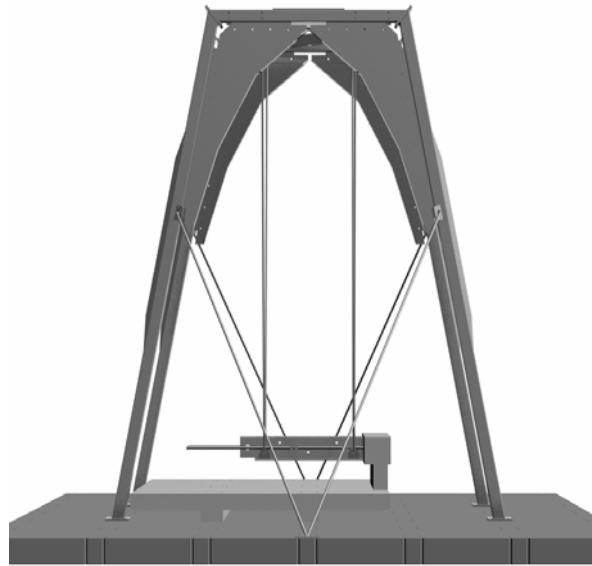*Figure B-2- Analytical model of pendulum support frame in SAP2000*

85

Figure B-3-Elevation rendering of impact test pendulum setup

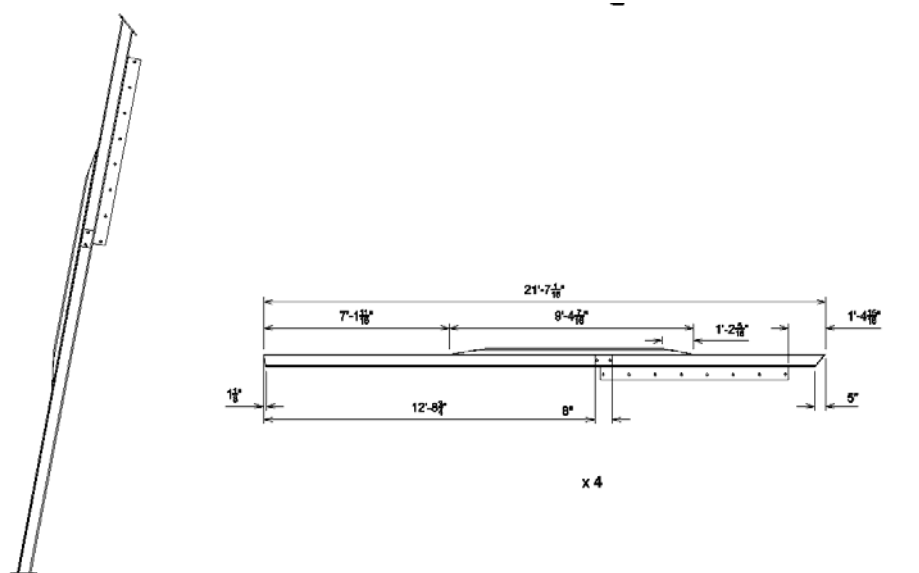**B.2** **SELECTED** **CONSTRUCTION** **DOCUMENTS** **FOR** **PENDULUM** **SUPPORT** **FRAME**

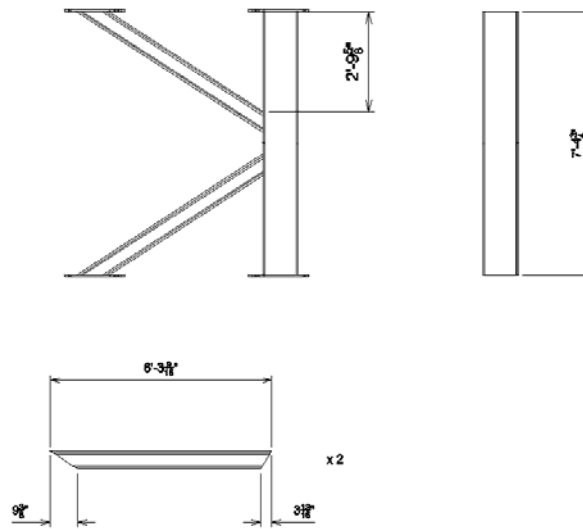*Figure B-4- Leg of pendulum support frame*

Figure B-5- Center K-brace of pendulum support frame
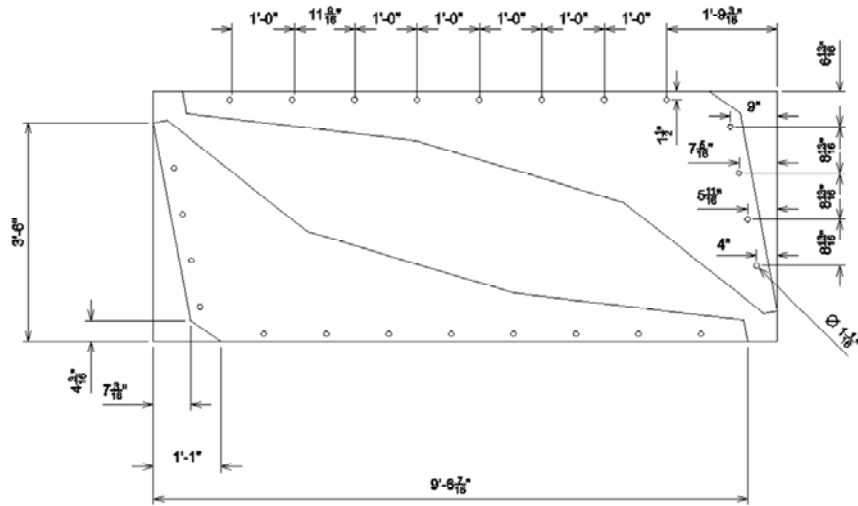

Figure B-6- Gusset plates for knee-braces, pendulum support frame
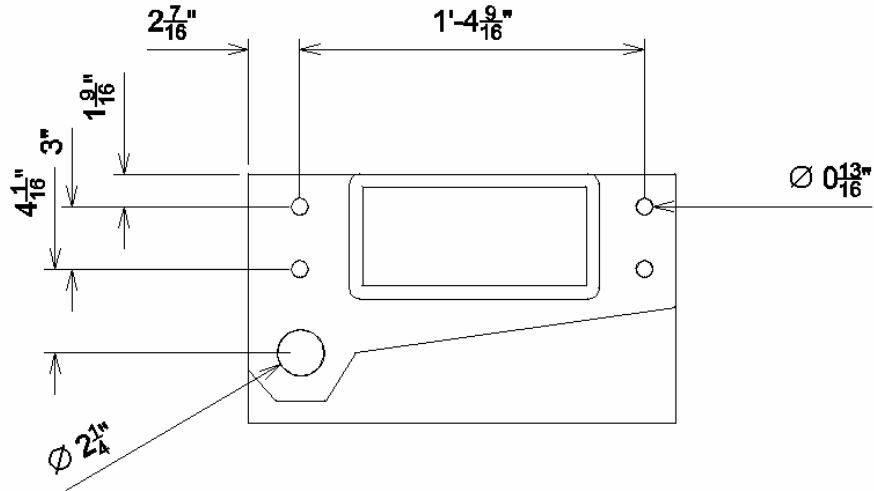
87

Figure B-7- Attachment plates for pendulum support cables

REFERENCES

ACI 318-05: ACI Committee 318, *Building Code Requirements for Structural Concrete (ACI 318-05)*, American Concrete Institute, Farmington Hills, MI.

(Bentley 2003): http://www.bentley.com.

(CSI Berkeley 2004): http://www.csiberkeley.com.

(Eligehausen and Sawade 1989): Eligehausen, R., and Sawade, G., "Fracture Mechanics Based Description of the Pull-Out Behavior of Headed Bolts Embedded in Concrete," *Fracture Mechanics of Concrete Structures: From Theory to Applications*, L. Elfgren, Ed., Chapman & Hall, London, 1989, pp. 263-281.

(Klingner 2003): Klingner, R., *"Behavior and Design of Fastening to Concrete,"* The University of Texas at Austin, September 2003.

(Livermore Software Technology Corporation 2005): http://www.lstc.com.

(MathWorks 2002): http/www.mathworks.com.

(NCHRP Report 350 1993): *NCHRP Report 350: Recommended Procedures for the Safety Performance Evaluation of Highway Features,* National Cooperative Highway Research Program, Transportation Research Board, National Research Council, National Academy Press, Washington, D.C.

(Tolnai 2005): Tolnai, Megan, *"Analytical Simulation of Vehicular Impact on Retrofit Bridge Barriers"*, Department of Civil, Architectural and Environmental Engineering, The University of Texas at Austin, May 2005.

(TTI 2002): Bullard, D. Lance Jr.; Williams, W. F.; Menges, W. L.; Haug, R. R., *"Design and Evaluation of the TxDOT F411 and T77 Aesthetic Bridge Rails,"* Report No. 4288-1 Texas Transportation Institute (TTI), Texas A&M University, College Station, Texas.,.

(TxDOT 2003): *Traffic Rail: Type T203,* Texas Department of Transportation, http://www.dot.state.tx.us/insdtdot/orgchart/cmd/cserve/standard/bridge-e.htm (accessed May 5, 2005).

VITA

Geoffrey Tyler Mitchell was born on August 2, 1979 in Milwaukee, WI, son of Jeffrey Parrick Mitchell and Laura Bauman Mitchell. Brother to Elliot Harrison Mitchell. He attended Westwood High School in Austin, Texas and graduated in 1997. After high school he enrolled in the University of Texas at Austin and, in May of 2003, was awarded the degree of Bachelor of Science in Architectural Engineering with honors. During his six years of undergraduate education he was a member of the Longhorn Band for two years and a rower for the UT rowing team for three. After graduation he received the NSPE Steinman Fellowship in recognition of academic excellence and high ethical standards. In September of 2003 he entered The Graduate School at The University of Texas to pursue a Master of Science degree in Engineering. While pursuing his graduate degree, he worked at the Ferguson Structural Engineering Laboratory as a Graduate Research Assistant under Dr. Richard E. Klingner and Dr. Eric B. Williamson.

Permanent Address: 11124 Callanish Park Drive

                                Austin, TX 78750

This thesis was typed by the author.